

This figure "Fig1.gif" is available in "gif" format from:

<http://arxiv.org/ps/astro-ph/0006412v1>

TABLE 1. Properties of UGC 7321

Hubble type: Sd IV
V_h : 407.2 ± 2.2 (km s ⁻¹)
Distance: 10_{-3}^{+3} (Mpc)
PA: 82°
i : 88°
a/b : 10.3
$D_{25.5}$: 5.6 (arcmin)
$A_{25.5}$: 16.3 (kpc)
$h_{r,B}$: $51'' \pm 4 \approx 2.5 \pm 0.2$ (kpc)
$h_{r,R}$: $43'' \pm 4 \approx 2.1 \pm 0.2$ (kpc)
$h_{r,H}$: $41'' \pm 3 \approx 2.0 \pm 0.1$ (kpc)
m_B : 13.84 ± 0.03
$B - R$: 0.99
$M_{B,i,0}$: -17.05
$\mu_{B,i}(0)$: 23.6 (mag arcsec ⁻²)
W_{20} : 233 ± 7 (km s ⁻¹)
\mathcal{M}_{HI} : $1.1 \times 10^9 (M_\odot)$
\mathcal{M}_{HI}/L_B : 1.1 (solar units)

Notes to Table 1.

Adopted distance is from Gallagher *et al.* (in preparation). Scale length measurements are described in Section 3. All other quantities are taken from Paper I. Apparent magnitudes and colors have been corrected for Galactic foreground extinction only. Absolute magnitudes, luminosities, and surface brightnesses were corrected for Galactic and internal extinction and projected to face-on values, as described in Paper I.

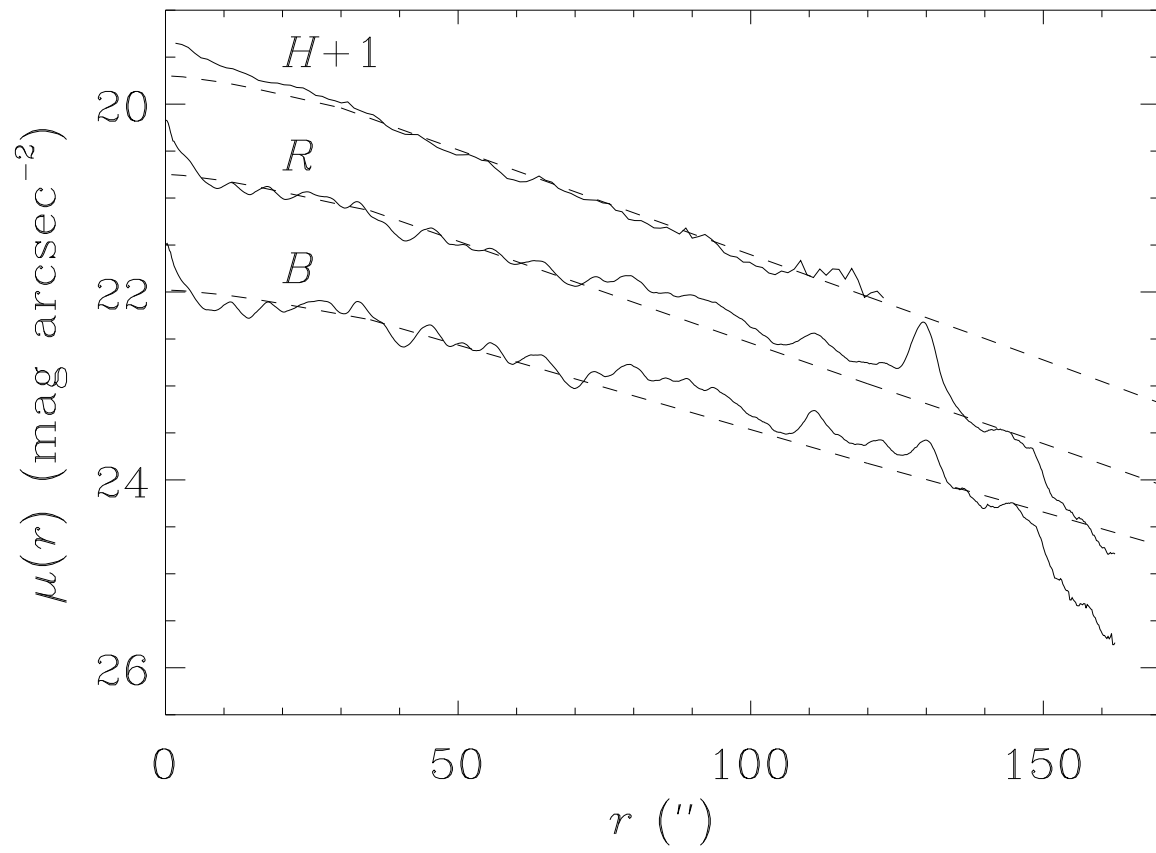
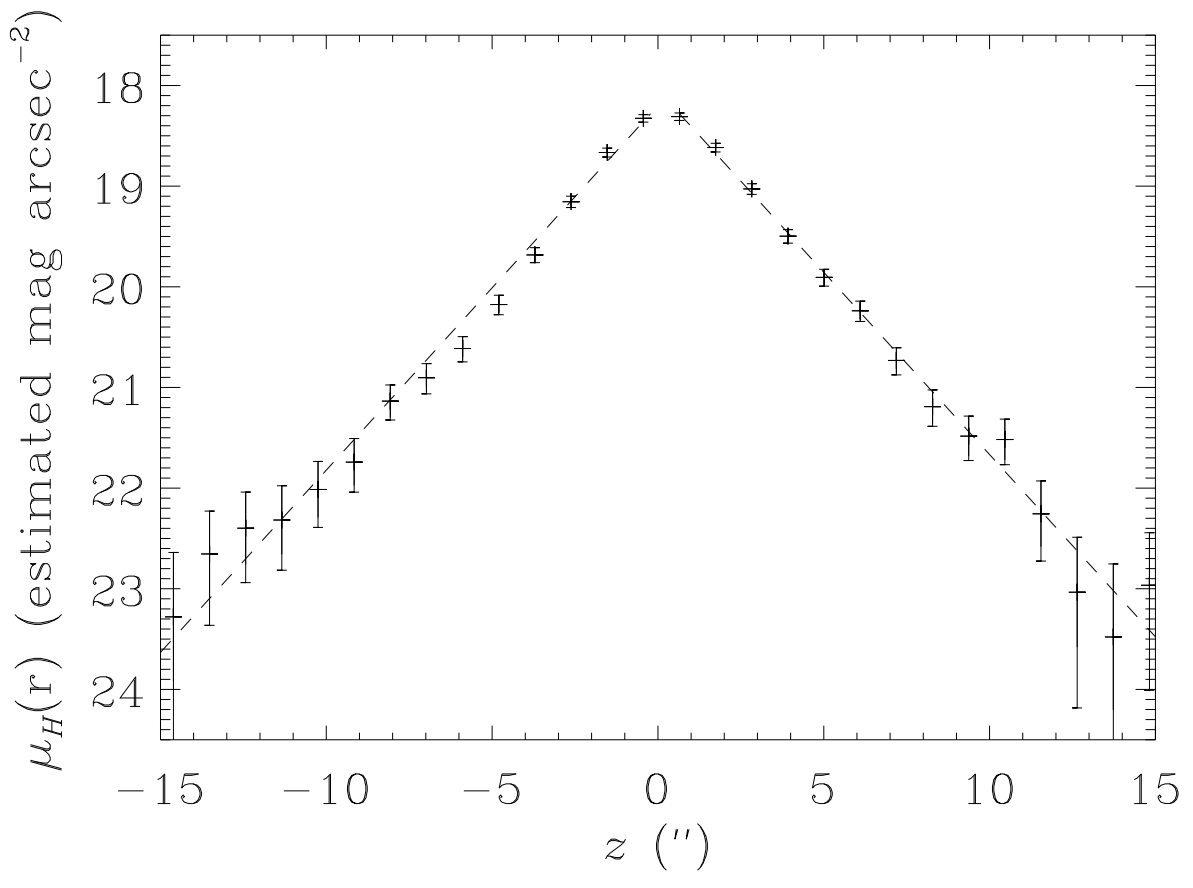


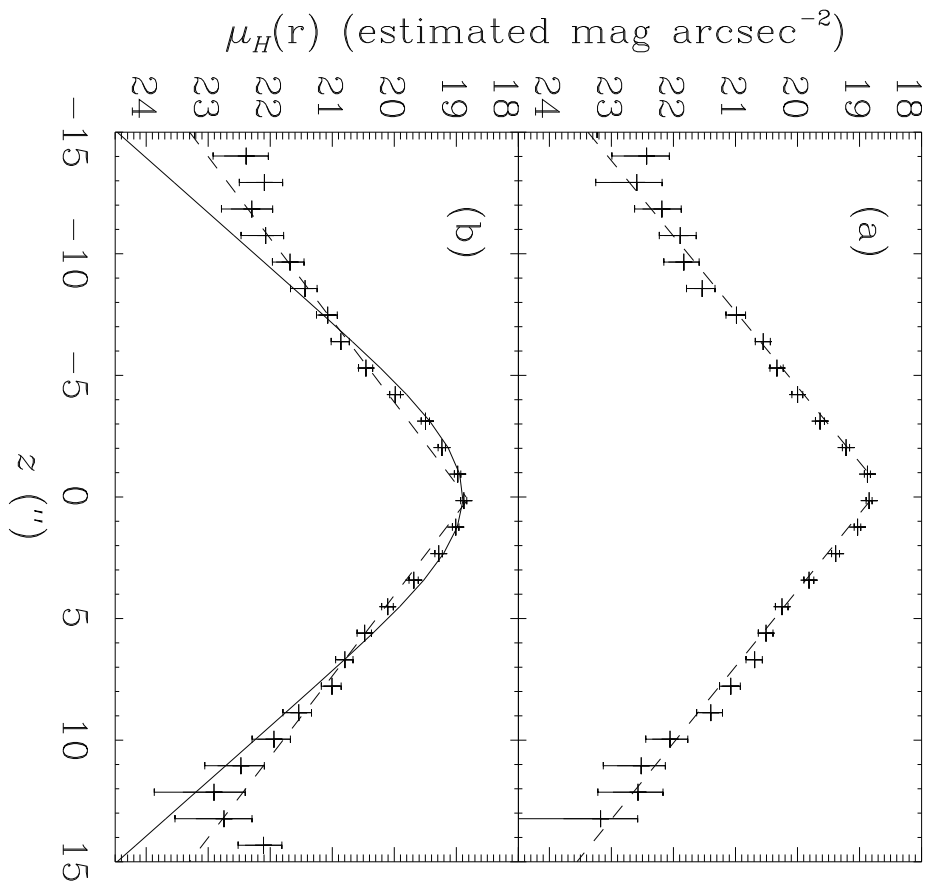
TABLE 2. Results from H -Band Single Component Vertical Profile Fitting

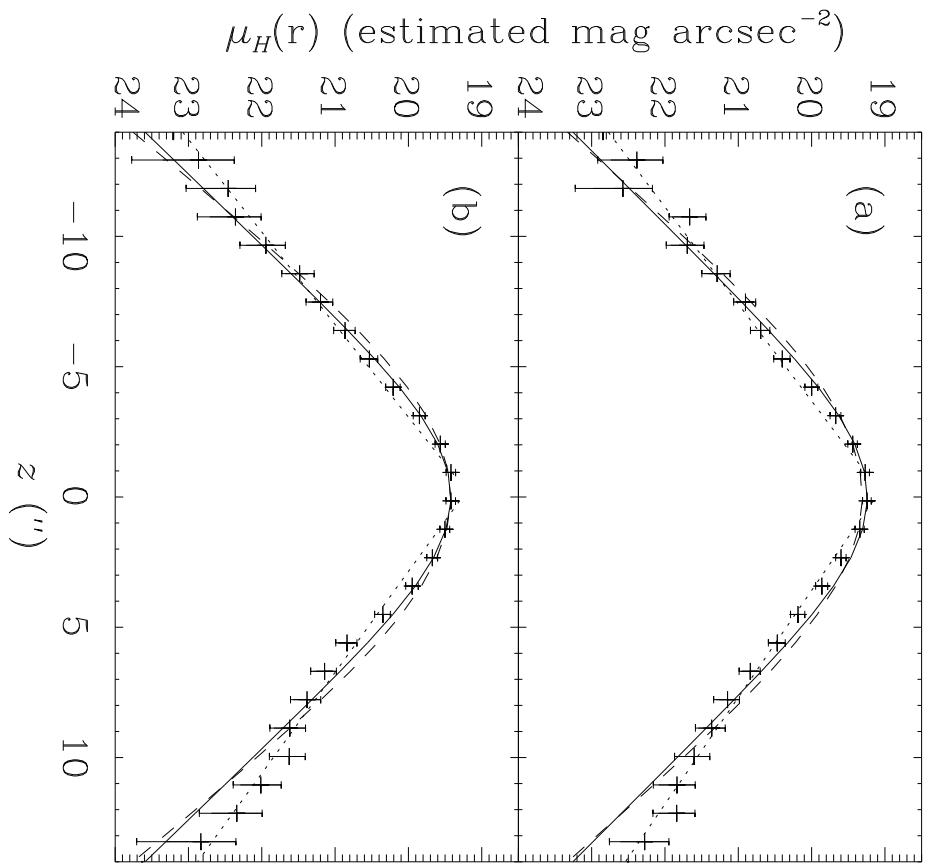
r (')	Function	\bar{h}_z (")	\bar{h}_z (pc)
+2.0	sech	4''.20	204
+1.5	sech	3''.61	175
+1.0	sech	3''.47	168
+0.5	sech	2''.95	143
+0'.25	sech	2''.45	119
+0'.25	exp	3''.63	176
0.0	exp	2''.87	139
-0'.25	exp	3''.40	165
-0.5	sech	3''.05	148
-1.0	sech	3''.66	186
-1.5	sech	4''.01	194

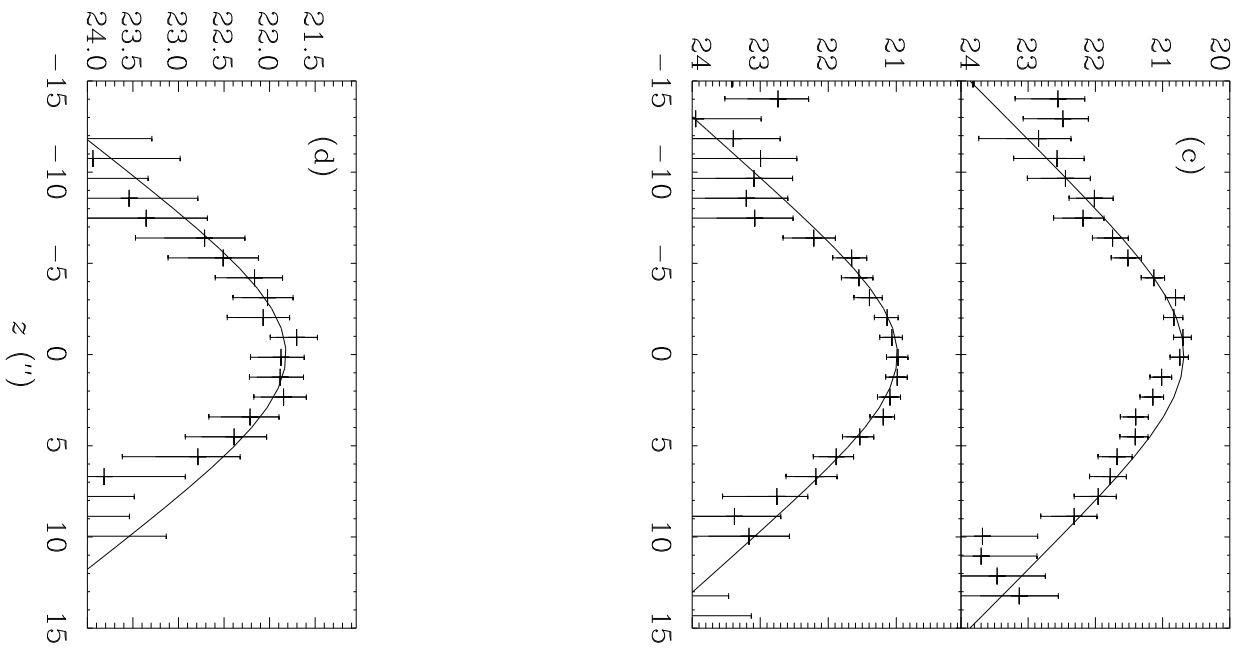
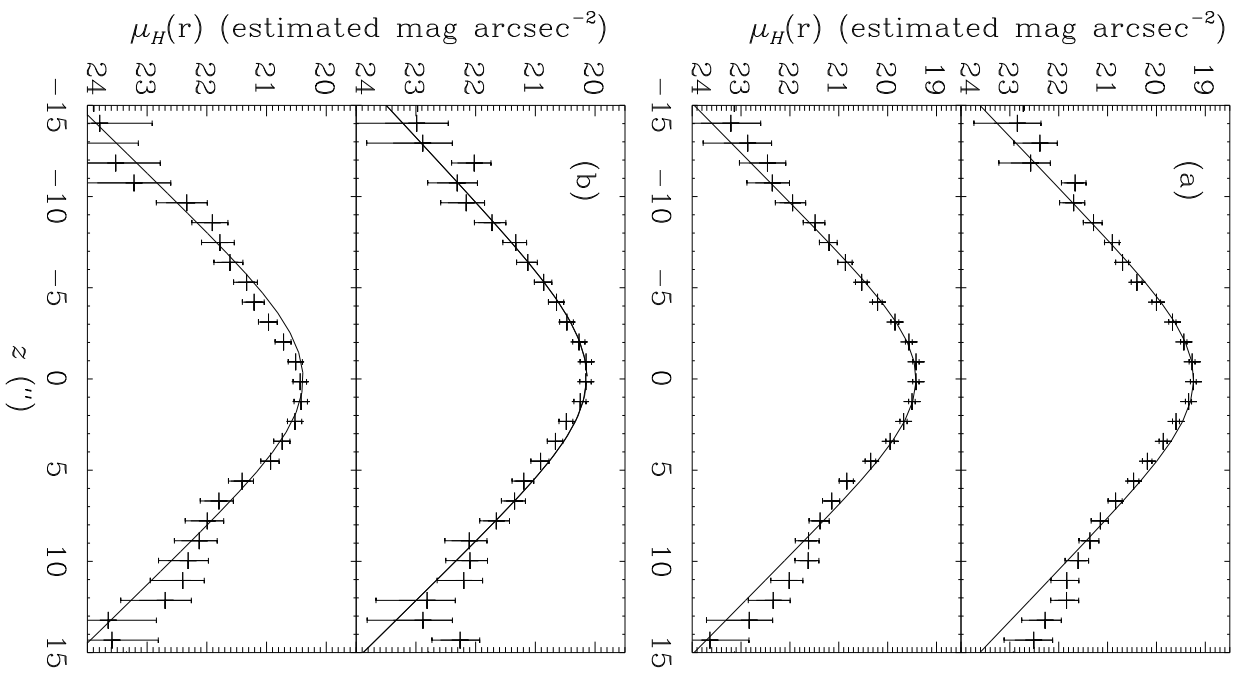
Notes to Table 2.

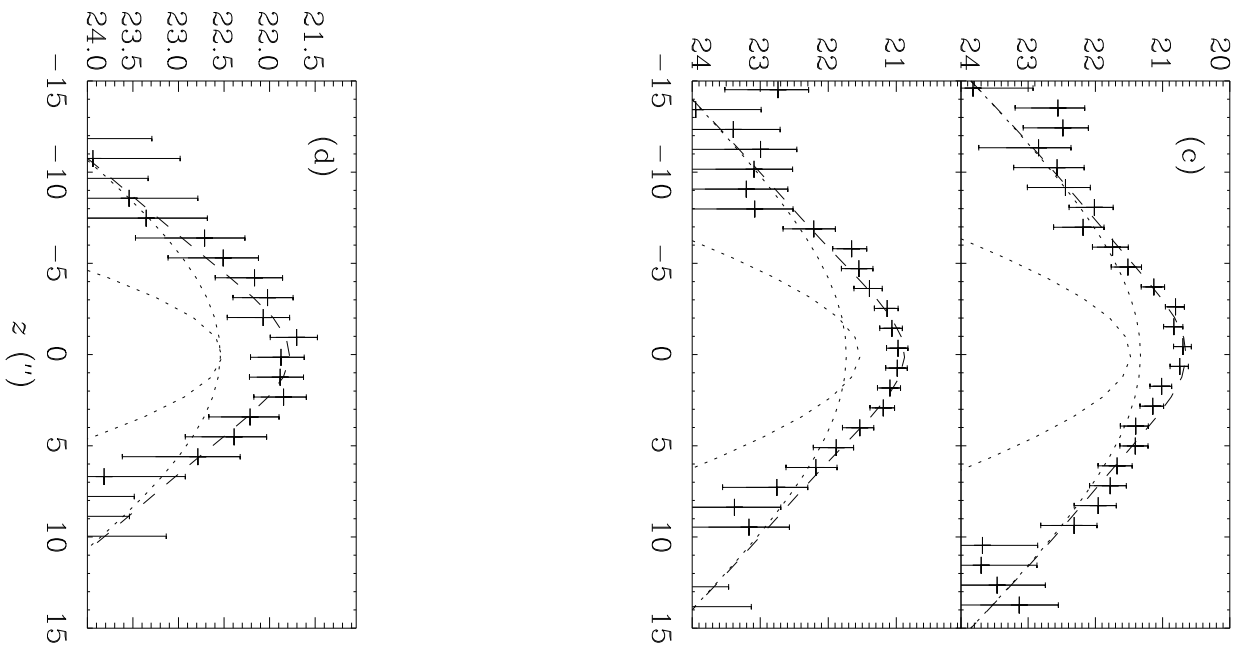
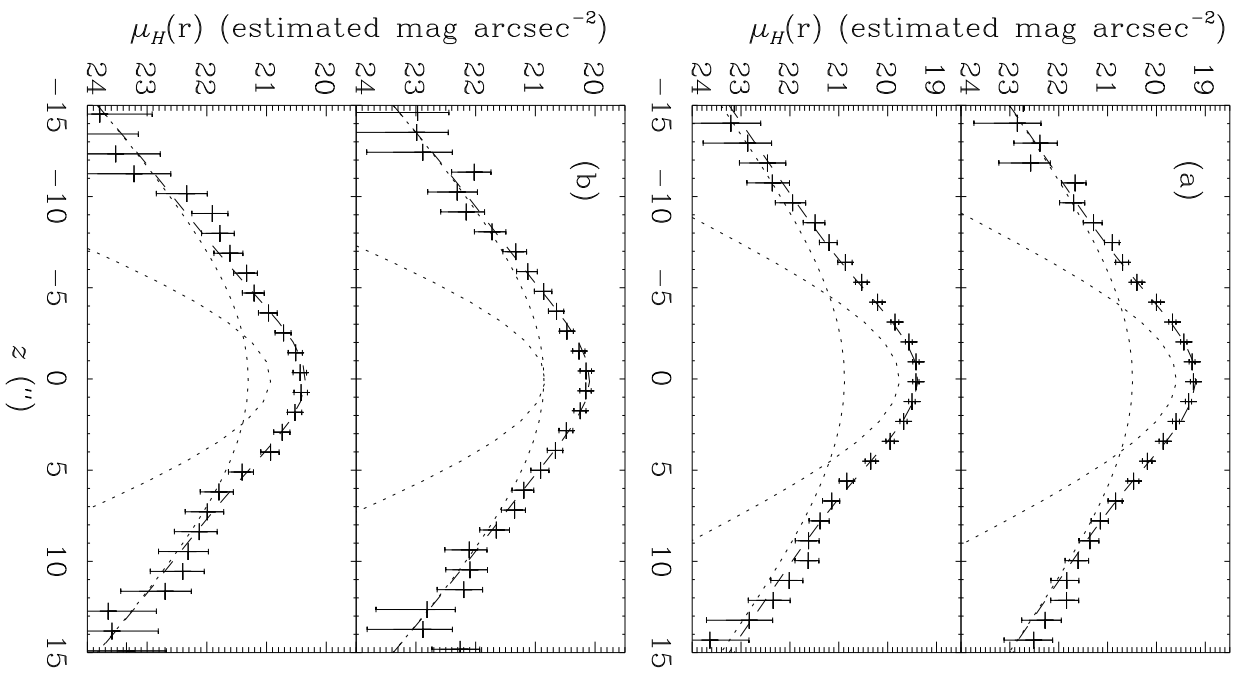
Quoted scale height values reflect the mean of the best fits on the $+z$ and $-z$ sides of the vertical profiles. Uncertainties in the individual scale heights are $\sim \pm 10\%$ (see Section 5). At $r = +0'.25$ the best single-component fit is intermediate between an exponential and a sech(z) function.

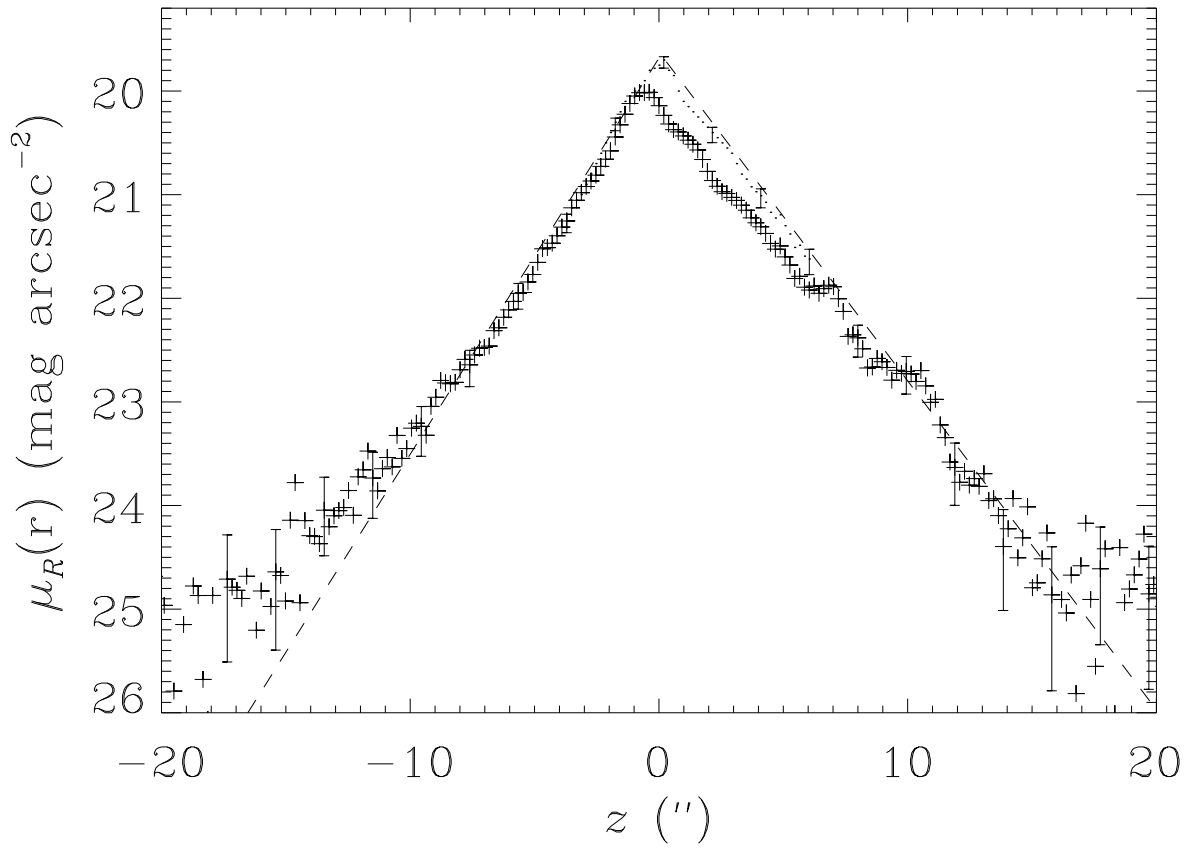


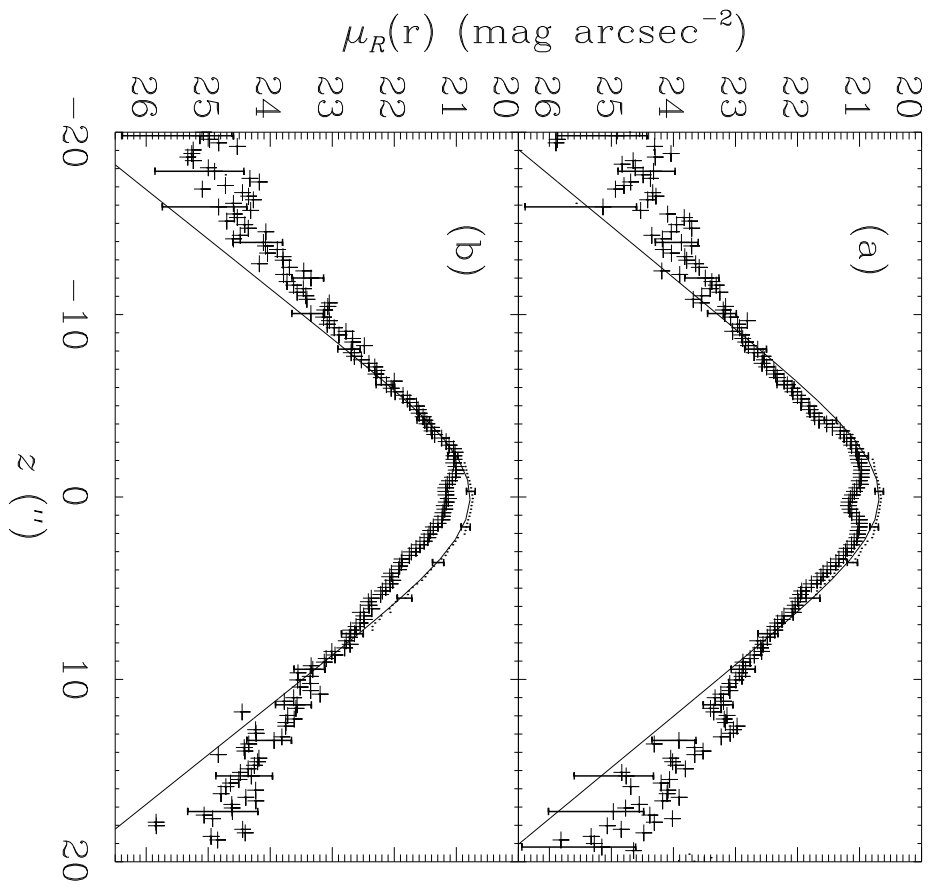


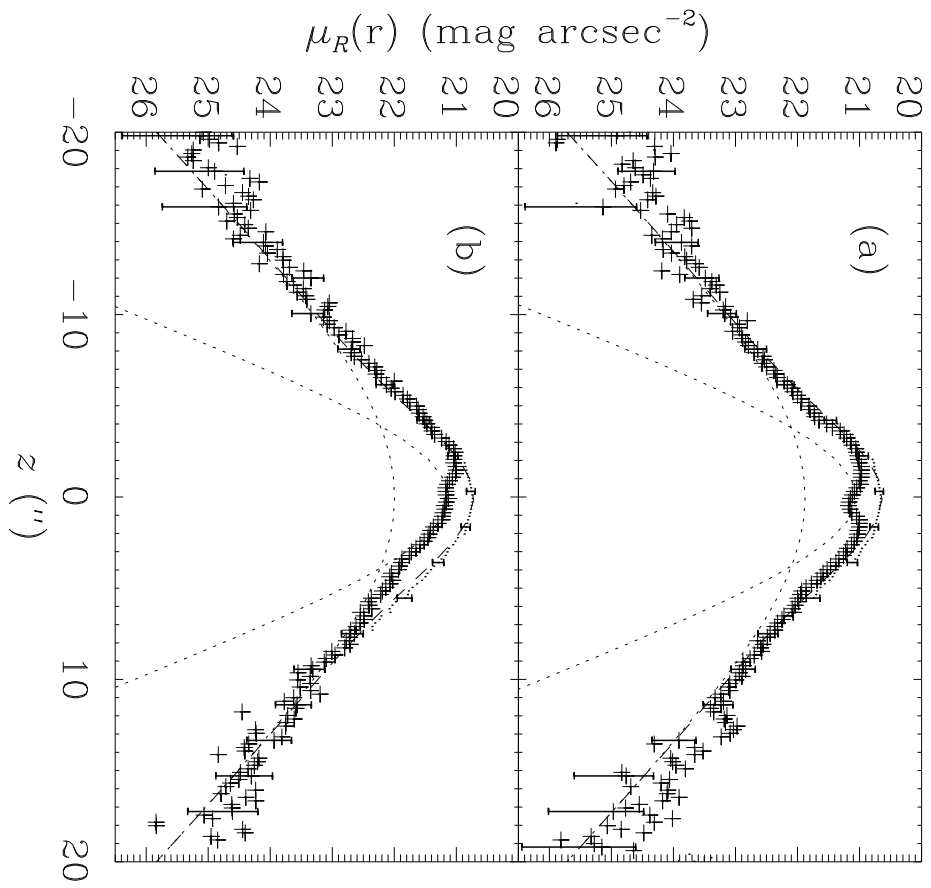


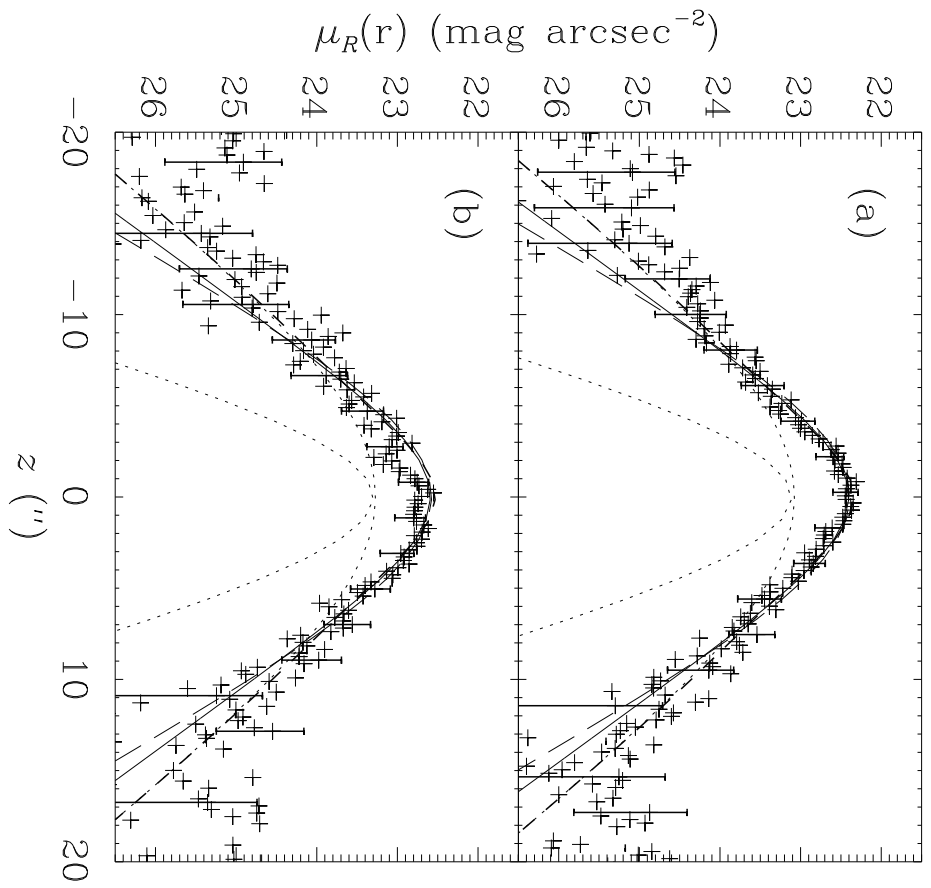












This figure "Fig12.gif" is available in "gif" format from:

<http://arxiv.org/ps/astro-ph/0006412v1>

The Extraordinary ‘Superthin’ Spiral Galaxy UGC 7321. II. The Vertical Disk Structure

L. D. Matthews¹

ABSTRACT

We explore the vertical light distribution as a function of galactocentric radius in the edge-on ($i=88^\circ$) Sd “superthin” galaxy UGC 7321. UGC 7321 is a low-luminosity spiral ($M_{B,i} = -17.0$) with a diffuse, low surface brightness stellar disk and no discernible bulge component. Within $\sim 0'.25$ (~ 725 pc) of the disk center the global luminosity profile of UGC 7321 can be reasonably characterized by an exponential function with a scale height $h_z \sim 2''.9$ (~ 140 pc) in H and $h_z \sim 3''.1$ (~ 150 pc) in R , making this among the thinnest galaxy disks known. Near the disk center we derive a ratio of disk scale length to global disk scale height $h_r/h_z \sim 14$ in both H and R ; near the edge of the disk, $h_r/h_z \sim 10$. At intermediate galactocentric radii ($0'.25 \leq |r| \leq 1'.5$), the disk of UGC 7321 becomes less peaked than an exponential near the galactic plane. At these radii the vertical luminosity profiles can be well reproduced by a linear combination of two isothermal disk components of differing scale heights. These fits, together with the strong disk color gradients by Matthews, Gallagher, & van Driel (1999), suggest that UGC 7321 has multiple disk subcomponents comprised of stellar populations with different ages and velocity dispersions. Thus even examples of the thinnest pure disk galaxies exhibit complex structure and signatures of dynamical heating.

Subject headings: galaxies: spiral—galaxies: structure—galaxies: evolution—galaxies: individual (UGC 7321)

1. Introduction

1.1. Background

Studies of the vertical light distributions of galaxy disks can offer vital clues toward understanding the physics and evolutionary histories of these systems. For example, vertical scale height measurements can be related to the stellar velocity dispersions and density profiles

¹National Radio Astronomy Observatory, 520 Edgemont Road, Charlottesville, VA 22903 USA, Electronic mail: lmatthew@nrao.edu

of disks, so constraints on their stability and dynamical evolution can be derived (e.g., Fuchs & Wielen 1987; Dove & Thronson 1993; Bottema 1993,1997; van der Kruit 1999a). When scale height measurements are combined with vertical color profiles, information can be gleaned on star formation histories and dynamical heating mechanisms (e.g., Just *et al.* 1996).

Van der Kruit & Searle (1981a,b;1982a,b; see also Spitzer 1942) proposed that galaxy disks could be modelled as self-gravitating locally isothermal sheets whose vertical light profiles $L(z)$ are described by

$$L(z) = L_o \text{sech}^2(z/z_0) \quad (1)$$

where L_o is the luminosity surface density, z is the vertical distance from the midplane of the galaxy, and z_0 is the scale height. In this model, the vertical velocity dispersion σ_z , is independent of z at a given galactocentric radius r .

Van der Kruit (1988) later argued that disks may deviate from isothermal near the galaxy plane, hence a better description of their overall vertical light profiles might be given as

$$L(z) = L_o \text{sech}(z/h_z) \quad (2)$$

which differs from a $\text{sech}^2(z)$ function only at small z . Here, $h_z = z_0/2$. This model has been applied successfully to fit the light distributions of some nearby galaxies (e.g., Barnaby & Thronson 1992; Rice *et al.* 1996).

As new and better data have become available in recent years, measurements of the vertical light distribution of our own Galaxy, as well as a number of external galaxies, have often pointed in favor of an exponential z light distribution of the form

$$L(z) = L_o \exp(z/h_z) \quad (3)$$

(e.g., Gilmore & Reid 1983; Pritchett 1983; Wainscoat, Freeman, & Hyland 1989; Aoki *et al.* 1991; van Dokkum *et al.* 1994; Barteldrees & Dettmar 1994; Kodaira & Yamashita 1996; de Grijs & Peletier 1997; Fry *et al.* 1999). Finally, de Grijs, Peletier, & van der Kruit (1997) have explored a more general family of fitting functions, which include relations 1-3 as special cases.

Part of the problem in distinguishing between these various relations empirically is that all of these functions look similar at large z values, while at small z the data are often contaminated by dust. There has also been little agreement on which of these relations should be favored on theoretical grounds. For example, it has remained poorly determined how each of these various distributions might be achieved physically, how the vertical structures of galaxy disks should be expected to change over time due to both internal and external processes, and to what degree the vertical structures of disks are determined by the initial conditions of formation (cf. Burkert & Yoshii 1996) versus subsequent evolution (e.g., Fuchs & Wielen 1987; Just *et al.* 1996). One way to gain insight into these issues is through detailed investigations of the vertical light distributions of galaxies spanning a range in properties.

To date, most detailed studies of the vertical structures of galaxies have concentrated on moderately luminous galaxies with normal surface brightness disks (e.g., de Grijs 1997 and references therein). Very few analyses (e.g., Kodaira & Yamashita 1996; Fry *et al.* 1999) have probed the vertical disk structures of the very latest spiral types, especially those with low luminosities and low optical surface brightness disks. However, the vertical structures of such “extreme late-type spirals” are of particular interest. For example, certain extreme late-type spirals appear to represent some of the least evolved nearby galaxy disks (e.g., Matthews & Gallagher 1997). Comparisons of their vertical structures with theoretical predictions can thus help to constrain evolutionary scenarios for these galaxies and allow us to determine how disk structure, dust contents, and dynamical evolution may differ between galaxy disks of high and low surface brightness. Because many extreme late-type and low surface brightness galaxies appear to be highly dark matter-dominated systems (e.g., Bothun, Impey, & McGaugh 1997 and references therein), vertical structure measurements of these systems combined with rotation curve and stellar velocity dispersion measurements may ultimately hold the key to unravelling the nature and distribution of dark matter in disk galaxies (e.g., Zasov, Makarov, & Mikhailova 1991; Bottema 1993,1997; Matthews 1998; Swaters 1999).

1.2. The Vertical Structure of a ‘Superthin’ Spiral

In a previous paper (Matthews, Gallagher, & van Driel 1999; hereafter Paper I), new multiwavelength data, including optical and near-infrared (NIR) imaging data, were presented for the edge-on “superthin” spiral UGC 7321. Here we utilize those datasets to probe the vertical luminosity distribution and vertical scale height of this galaxy over a range of galactocentric radii.

Visual inspection alone reveals some of UGC 7321’s most interesting traits: a diffuse stellar disk, large disk axial ratio, and complete absence of a discernible bulge component (Fig. 1). Some additional properties of UGC 7321 are summarized in Table 1. The distance quoted in Table 1 (10_{-3}^{+3} Mpc) is estimated from resolved luminous stars in imaging data obtained with the *Hubble Space Telescope* (Gallagher *et al.*, in preparation). This distance is twice that estimated by Tully, Shaya, & Pierce (1992) based on galaxy group assignments and peculiar motion analyses, indicating that UGC 7321 appears to be a rather isolated system, and is unlikely to have undergone any recent perturbations.

In Paper I it was shown that UGC 7321 has a low optical surface brightness disk that exhibits significant radial and vertical color gradients, and that it suffers relatively minimal internal extinction due to dust. Together these trends were interpreted as evidence that UGC 7321 is highly “underevolved” disk in both a dynamical and in a star-formation sense. Therefore it is of tremendous interest to compare the vertical structure of this seemingly “primitive” galaxy with that of more “normal” spirals. Fortunately the nearly edge-on geometry of UGC 7321 ($i \approx 88^\circ$) makes it ideally suited for such an analysis.

2. The Data

Optical and NIR imaging observations are complementary for the analysis of the vertical density structures of galaxies. NIR images have the advantage that they are considerably less affected by dust than optical data, so the effects of internal extinction on the observed brightness distribution are minimized and the vertical light distribution can be probed even at very small z -heights. In addition, the light contribution from recent star formation is lower in the NIR, so NIR light profiles of galaxies should give the best measure of the radial and vertical distribution of the underlying older stellar populations. Unfortunately, due to the high NIR sky background, NIR observations are generally of lower signal-to-noise than CCD observations at optical wavelengths, particularly for very low surface brightness galaxies. It is therefore more difficult to trace the light profiles of galaxies in the faintest outer disk regions or at large z heights in the NIR. However, optical observations can be used to supply supplemental information in these regimes, since dust extinction is usually minimal in those regions. Moreover, comparisons of galaxy scale heights and scale lengths measured in multiple wavebands can supply important information about disk evolution and star formation histories. For these reasons, we undertake the analysis of the vertical structure of the UGC 7321 disk utilizing both H -band and R -band imaging observations. Details regarding the acquisition and reduction of these data can be found in Paper I.

3. Radial Scale Length Measurements

In Paper I, a radial disk scale length for UGC 7321 was reported for the B -band only. Here we rederive this measurement using an alternate technique. We also measure scale lengths in the R and H bands for subsequent comparison with our vertical structural measurements at these wavelengths.

As is well known, accurately measuring scale lengths for galaxy disks can be a difficult task, and the numbers derived can vary greatly depending on the technique used and the limiting isophote of the data (e.g., Knapen & van der Kruit 1991). In Paper I, a B -band radial scale length of $44'' \pm 2''$ was derived for UGC 7321 using isophotal fits. This technique has the advantage of maximizing signal-to-noise for obtaining a global disk scale measurement, although as was noted in Paper I, the validity and accuracy of this technique begins to break down for galaxies viewed very near edge-on. The result can be a tendency to slightly underestimate the true disk scale length in the nearly edge-on case (see also de Grijs 1998).

An alternate method for measuring the radial scale lengths of edge-on galaxies is through fits parallel to their major axis light profiles. We adopt this technique in the present work.

Our data were first processed as described in Sect. 4.1 below. We then extracted light profiles along the major axis from the B -, R -, and H -band data. The extracted profiles were 12-pixels thick in B and R and 3 pixels thick in H . Often a light profile is extracted slightly offset from

the true major axis in order to avoid the effects of dust (e.g., Wainscoat, Freeman, & Hyland 1989; Barteldrees & Dettmar 1994; de Grijs 1998). Unfortunately, because the UGC 7321 disk is so thin, this is not possible in the present case. To increase signal-to-noise, we folded each of the radial profiles about $r=0$, and in the case of the R - and B -band data, we have also smoothed the profiles by a factor of 15 along the radial direction. The resulting surface brightness profiles are shown in Fig. 2. As our H -band data are not photometrically calibrated, throughout this paper we illustrate these data using an absolute surface brightness scale estimated from a comparison with the photometrically-calibrated Two Micron All Sky Survey (2MASS) H -band data for UGC 7321².

To determine the scale lengths, we fitted each of the profiles in Fig. 2 using Eq. 5-9 of van der Kruit & Searle (1981a; see also Paper I). The best fits were determined by eye and are overplotted on Fig. 2 as dashed lines. Our derived measurements are as follows: $h_{r,H} = 41'' \pm 3''$, $h_{r,R} = 43'' \pm 4''$, and $h_{r,B} = 51'' \pm 4''$. The differences as a function of wavelength reflect the radial color gradients present in the disk of UGC 7321 (see Sect. 6.1.1; see also Paper I).

From Fig. 2 it can be seen that a pure exponential provides only an approximate fit to the data. Possible implications of this are discussed further in Paper I. Because the disk of UGC 7321 is rather diffuse, even our smoothed, folded profiles are not very smooth at optical wavelengths. In addition, a light excess (discussed further in Paper I) is seen at small radii, particularly in the H band, while at large radii ($r \approx 150''$) it appears the disk may be truncated. Finally, over the interval $70'' \leq r \leq 130''$, Fig. 2 shows there is also a light excess visible in both the B and R bands.

4. Vertical Structure Measurements

4.1. Extraction of the Vertical Light Profiles

We explored the vertical structure of the UGC 7321 disk by examining one-dimensional cuts extracted from our H - and R -band images at a variety of galactocentric radii. Before extracting the light profiles, the images were sky-subtracted and the IRAF³ task “imedit” was used to remove cosmic rays, field stars, and background objects in the vicinity of the galaxy. Using field stars as a reference, we found the peak central brightness of UGC 7321 to occur in identical locations in both the H and the R frames, and defined this to be the galaxy center ($r=0$).

Beginning at $r=0$, we extracted 3- and 15-pixel ($\sim 3''$) wide cuts parallel to the galaxy minor axis from the H and R images, respectively, at 0:25-0:5 intervals along the galaxy. A position angle of 172° for the galaxy minor axis was adopted. The locations of the extracted cuts are illustrated in Fig. 1. Throughout this paper we use z to denote the distance above or below the

²The Two Micron All Sky Survey photometric parameters were accessed through <http://sirtf.jpl.nasa.gov/2mass/>.

³IRAF is distributed by the National Optical Astronomy Observatories, which is operated by the Associated Universities for Research in Astronomy, Inc. under cooperative agreement with the National Science Foundation.

galaxy midplane, and r to denote the distance from the disk center. For clarity we adopt the convention that r is positive on the eastern (E) side of the disk, and negative on the west (W) side, rather than the usual cylindrical coordinates.

The widths of the extracted strips were selected to obtain reasonable signal-to-noise without sacrificing the ability to discern changes in scale height or disk structure as a function of radius. Because in H -band, our pixel size ($1''.09$) is non-negligible compared with the thickness of the UGC 7321 disk, no binning was applied to the cuts along the vertical direction; pixels in the optical data are smaller ($0''.195$), but still no vertical binning was applied due to the very steep slope of the light profiles.

4.2. Gauging the Effects of Dust

An important consideration in analyzing the vertical light structures of galaxies is accounting for the effects of internal dust absorption on the observed light distribution. Our optical data (Paper I), as well as R and I images of UGC 7321 obtained with the *Hubble Space Telescope* (Gallagher *et al.*, in preparation) reveal that UGC 7321 clearly contains dust, although this galaxy lacks the quintessential dust lane found in most brighter spirals viewed edge-on (cf. Howk & Savage 1999). The dust distribution in UGC 7321 instead appears patchy and clumpy, and cannot be well approximated by a uniform layer (see also Matthews & Wood, in preparation).

Fortunately for our purposes, the bulk of the dust in UGC 7321 appears to be confined to a region along the galaxy midplane only a few arcseconds thick ($-3'' \lesssim z \lesssim 7''$). This can also be seen in our R -band vertical cuts (e.g., Fig. 8-10, discussed below), where indentations due to dust are visible. The slight asymmetry of these features about $z=0$ confirms that UGC 7321 is not viewed exactly edge-on, but rather at an inclination $i \approx 88^\circ$ (see also Paper I).

In H -band, the effects of dust appear to be essentially negligible in UGC 7321. None of our H -band profiles exhibit obvious indentations due to dust (see Fig. 3-7, discussed below) and the H -band contours show no evidence for the type of asymmetries or irregularities expected from dust absorption (see Fig. 2 of Paper I). For these reasons, and because of the patchy distribution of dust in UGC 7321, in the present work no effort was made to model its effects on the light profiles in a sophisticated manner. Effects of dust were therefore ignored in the H -band, while in the R -band, dust at small z was compensated for by a simple extrapolation of the profiles from intermediate z regions (see also Kodaira & Yamashita 1996). The dust distribution of UGC 7321 and its detailed effects on the observed properties of UGC 7321 have recently been investigated by Matthews & Wood (in preparation) using three-dimensional Monte Carlo radiation transfer models. These sophisticated models confirm that dust effects in H -band are quite small and that the simple dust treatment we adopt here is adequate for our present purposes.

4.3. The Fitting Technique

Using a nonlinear least squares fitting technique based on the CURFIT program of Bevington (1969), we attempted fits to the extracted vertical luminosity profiles with each of the three functions given by Eq. 1-3 (hereafter the ‘ $\text{sech}^2(z)$ ’, ‘ $\text{sech}(z)$ ’, and ‘exponential’ functions). These respective functions were convolved with a Moffat function (Moffat 1969) before fitting in order to mimic the effects of seeing on the model light profiles. The Moffat function is given as

$$p(r) = \frac{\beta - 1}{\pi\alpha^2} \left[1 + \left(\frac{r}{\alpha} \right)^2 \right]^{-\beta} \quad (4)$$

with

$$\text{FWHM} = 2\alpha\sqrt{2^{1/\beta} - 1}, \quad (5)$$

where α was solved for in each case. We assumed $\beta=2.5$ (Saglia *et al.* 1993), and the FWHM for a point source in each band was determined using the mean value from fits to several stars in each field.

Each point in the light profiles was weighted during fitting by a term that accounted for Poisson noise and sky and flatfield uncertainties. Initially, the profiles on either side of the midplane [hereafter the $+z$ (north) and $-z$ (south) sides] were fitted independently. This permitted us to search for systematic difference in shape or scale height of the two sides of the profile and provided a means of estimating the uncertainty in the fits (see below).

For each fit it was necessary to supply initial guesses for the parameters L_o and z_0 (or h_z). The fitting program then used a chi-squared minimization technique to find an acceptable fit. Refined values of L_o and z_0 (or h_z) were then inputted, and the process was repeated for several iterations before converging at a final solution. All fits were also compared with the data by eye as a second check of fit optimization. To ensure proper handling of errors, the fitting was initially performed in linear rather than magnitude space.

4.4. Fitting Round 1: The H -Band Data and One-Component Models

To minimize any impact from dust and small-scale star-forming complexes, we performed a first round of fits on the H -band profiles. Our H -band data have sufficient signal-to-noise and field-of-view to permit fits to the vertical profiles over the disk region $-1'.5 \leq r \leq +2'.0$. Each individual profile was fitted over the interval $-20'' \leq z \leq +20''$, which was found by trial and error to optimize the quality and stability of the fits. From the initial set of fits to the H -band data, several interesting features of the vertical light distribution of UGC 7321 became apparent.

Fig. 3 illustrates the best fit along the disk minor axis ($r=0$). At this location, the H -band vertical light profile is too strongly peaked at small z values to be reproduced by either a $\text{sech}(z)$ or $\text{sech}^2(z)$ function. However, the profile can be reasonably well reproduced over the full range

of z by a single exponential function with a scale height $h_{+z,c}=3''.0$ on the $+z$ side of the galaxy and $h_{-z,c}=2''.74$ on the $-z$ side. At the adopted distance of UGC 7321 this corresponds to a mean scale height of $\bar{h}_{z,c} \approx 140$ pc. *This is one of the smallest global vertical scale heights ever reported for a galaxy disk.*⁴ For example, this is less than half the global exponential scale height of the Milky Way disk ($h_z \approx 300$ pc; e.g., Freeman 1991).

Moving slightly away from the disk center, at $r = -15''$ we find the H -band light profile is still well fit by an exponential, but with a slightly larger mean scale height ($\bar{h}_{z,-15''}=3''.4$) than measured at $r=0$ (Fig. 4a). However, on the opposite side of the disk, at $r = +15''$, an exponential with $\bar{h}_{z,+15''} = 3''.63$ fits the data nicely at large z , but at small z this function is seen to be somewhat too strongly peaked to reproduce the data (Fig. 4b). On the other hand, a $\text{sech}(z)$ function with $\bar{h}_z=2''.45$ is slightly too rounded at small z , and leaves residuals in the profile wings. Because of the exponential nature of the profiles at $r=0$ and $r = -15''$, this deviation from an exponential cannot easily be attributed to inclination, seeing, or resolution effects. Moreover, we see this trend become more pronounced as we move to larger galactocentric radii.

At $r = \pm 0'.5$ we again find that the light profile can be fit by an exponential at large z , but at small z , the exponential is clearly too strongly peaked to fit the data (Fig. 5). Instead, at small z values the shape of the light profile is better reproduced by either a $\text{sech}(z)$ or a $\text{sech}^2(z)$ function, with the $\text{sech}(z)$ giving the best overall fits.

At larger galactocentric radii, the $\text{sech}(z)$ function continues to provide the best global fits to the H -band data over the full range of z . The results of these fits are shown in Fig. 6. Table 2 summarizes the mean derived scale heights h_z from the one-component fits at various galactocentric radii.

The numbers in Table 2 seem to suggest that the scale height of the UGC 7321 disk increases with radius by over 30% in the interval $-1'.5 \leq r \leq -0'.5$, and by over 40% in the interval $+0'.5 \leq r \leq +2'.0$. As discussed in Sect. 5, we estimate the errors in our single-component model fits to be $\sim \pm 10\%$, hence this increase is statistically significant.

In general, disk scale heights of late-type spiral galaxies are found to increase by no more than a few per cent with radius (e.g., de Grijs & Peletier 1997), hence the large increase we measure for UGC 7321 is surprising. One possibility is that there is significant flaring in the outer disk due to decreasing self-gravity (see also Capaccioli, Vietri, & Held 1988). Another possibility is that the one-component $\text{sech}(z)$ model fits are not adequate to describe the data at all z heights due to the presence of an additional disk component. While the first possibility likely makes some contribution to the trends we observe (see also Sect. 6.1.2), as we show below, it indeed also

⁴Using NIR data, Kodaira & Yamashita (1996) measure a global scale height of $h_z = 158$ pc for the pure-disk, edge-on galaxy NGC 4244, making this one of the few reported values comparable to that which we measure for UGC 7321. However, Fry *et al.* (1999) report a larger global exponential scale height for NGC 4244 in the R band ($h_z=246$ pc).

appears that the UGC 7321 structure is more complex than indicated by a simple, one-component model.

4.5. Fitting Round 2: The H-band Data and Two-Component Models

In Fig 5& 6, it is clear that while the $\text{sech}(z)$ fits can be argued to provide a reasonable, rough global characterization of the light profile shapes, they fall short of completely reproducing the observed light profiles to within the observational errors over the full range of z . In particular, in the $r = \pm 0.5$ and $r = \pm 1.0$ profiles, where signal-to-noise is high, small light excesses are visible in the data at $|z| \gtrsim 9''$, especially on the $+z$ side of the disk. These excesses suggest that a second fit component may be necessary to fully reproduce the observed vertical light distribution of UGC 7321.

To test this possibility, in Fig. 7a & b we show revised fits to the H -band light profiles of UGC 7321 at $r = \pm 0.5$, this time using a linear combination of *two* $\text{sech}^2(z)$ components of differing scale heights⁵. To derive the fits shown, we initially fitted the $+z$ and $-z$ halves of each profile independently. By using a mean of these results, we arrived at a simple, two-component $\text{sech}^2(z)$ model that provides an excellent and improved fit to the data over the full range of z . In these fits, the scale height of the inner fit component was taken to be $z_{0,1} = 3''.8$ (185 pc) and the scale-height of the outer component was taken to be $z_{0,2} = 8''.7$ (423 pc). The relative light contributions of the two components were the same on both the E and W sides of the disk. Only a small difference in scaling of the total profile was necessary to account for the slightly different peak brightnesses on the two sides.

Even though we have used mean fit values in Fig 7, the two-component fits still show a clear improvement over the single-component $\text{sech}(z)$ models shown in Fig. 6. Both the inner points and the profile wings are now reproduced to within their error bars over the interval $-15'' \leq z \leq +15''$.

To test the statistical significance of the improvement produced by the extra light component in these new models, we have applied a statistical F test to compare the two fits (e.g., Bevington 1969; Chatterjee & Price 1977). Following Chatterjee & Price (1977), the F ratio applicable to determining the significance of additional fit terms is defined as

$$F = \frac{[\chi^2(1) - \chi^2(2)] / (p + 1 - k)}{\chi^2(2) / (n - p - 1)} \quad (6)$$

where $\chi^2(1)$ characterizes the “full model” with $(p + 1)$ free parameters [here the two- $\text{sech}^2(z)$ model], $\chi^2(2)$ characterizes the “reduced model” with k distinct parameters [here the $\text{sech}(z)$ model], and n is the number of data points fitted.

⁵Linear combinations of two $\text{sech}(z)$ components also provide similarly good fits to the data (see Sect. 5).

For this test, we presently limit ourselves to the interval $-15'' \leq z \leq +15''$. At $r = -0'.5$, for the 29 fitted data points, we derive $\chi^2(1)=42.94$ and $\chi^2(2)=11.79$. At $r = +0'.5$, for the 25 fitted data points, $\chi^2(1)=18.72$ and $\chi^2(2)=7.34$. From the F distribution probability table of Abramowitz & Stegun (1965; Table 26.9), we infer that in both instances there is a $> 99.9\%$ probability that these second fit components are warranted. From this we deduce that *at moderate galactocentric radii, the disk of UGC 7321 is not strictly isothermal or sech(z)-like over its full z-extent, but rather has a more complex structure.*

Over the full interval $-1'.5 < r \leq +1'.5$, we continue to find that the two-component model comprised of two $\text{sech}^2(z)$ functions of scale heights $z_{0,1} = 3''.8$ and $z_{0,2} = 8''.7$, respectively, produces superior fits to the data compared with the single-component $\text{sech}(z)$ fits, based on both the F statistic (at the $> 90\%$ certainty level) and visual inspection, provided that the relative contribution to the total fit of the larger z -height component is allowed to increase with increasing galactocentric radius. A slightly more significant increase in the contribution of the higher z -height component was required on the W side of the galaxy than on the E side (see Fig. 7). We discuss possible implications of this further below. Over this interval we find no evidence for scale height changes in either component to within errors, although we cannot rule out changes of $\lesssim 10\%$. Only at $r = +1'.5$ and $r = +2'.0$ do the $\text{sech}(z)$ models and the two-component $\text{sech}^2(z)$ models become formally indistinguishable in the H -band (see also Sect. 4.6&6.1.1).

4.6. Fitting Round 3: R-Band Fits

As was shown above, over the interval $15'' \lesssim |r| \lesssim 1'.5$, the H -band light profiles perpendicular to the UGC 7321 disk are best reproduced over their full z extent by a model comprising a sum of at least two light components. Before interpreting this result further, we need to first explore the possibility that the requirement for a second light component is simply an observational artifact due to scattered light or flatfielding problems in the H -band data. Since the signal-to-noise of the R -band data is superior to that of the H -band data at large z values and at large r , these data can be used to provide a check on the results obtained at H -band.

We began by attempting to fit the vertical R -band profile at $r=0$ in the manner described above, successively using single exponential, $\text{sech}(z)$, and $\text{sech}^2(z)$ functions. As described above, our R -band data were corrected for dust at small z -heights by using an extrapolation of the light profile from intermediate z . Because of the clumpy nature of the dust in UGC 7321, this procedure is uncertain at any given location to $\sim \pm 0.3$ mag arcsec $^{-2}$. As with the H -band, fits in the R -band were performed over the interval $-20'' \leq z \leq +20''$.

The results of the R -band fits at $r=0$ are shown in Fig. 8. It can be seen that after dust is accounted for, the R -band vertical light profile of UGC 7321 is reasonably reproduced over a large range in z by a single exponential function of scale height $h_{-z,c,R} \approx 2''.84$ on the $-z$ side of the profile and $h_{+z,c,R} \approx 3''.42$ on the $+z$ side, for a mean of $\bar{h}_{z,c,R} \approx 152$ pc. These values are slightly

larger than derived in the H -band, although the difference is only marginally significant to within expected errors (see Sect. 5). Note however that there is possible evidence of some faint residuals to our fits at $\mu_R \geq 23.7$ mag arcsec $^{-2}$ ($\sim 3\%$ of sky), particularly on the $-z$ side of the profile. Careful inspection of the H -band minor axis profile (Fig. 3) shows that such residuals may also be marginally present in these data. We return to this point in Sect. 6.1.3.

At larger galactocentric radii, we find that as with the H -band data, the dust-corrected R band vertical cuts cannot be characterized over the full range of z values by a single exponential, $\text{sech}(z)$, or $\text{sech}^2(z)$ function. In Fig. 9 we show the R -band vertical profiles at $r = \pm 0'.5$ with the H -band single-component $\text{sech}(z)$ fits from Fig. 6a overplotted. The residuals initially seen in the H -band fits are now far more pronounced, occurring at R -band surface brightness levels of $\gtrsim 22.8$ mag arcsec $^{-2}$, or roughly 6% of sky. Due to dust, at very small z -heights we are unable to ascertain how intrinsically peaked the R -band light profile is near the galaxy midplane. However, even taking into account the uncertainties of the dust corrections, it is clear that no one-component model can reproduce the data over the full range of z . Our R -band fits thus give a second strong piece of evidence for the need for a second model component to fully reproduce the data.

Fig. 10a & b again show the observed R -band vertical brightness cuts at $r = \pm 0'.5$, but this time overplotted are scaled versions of the two-component $\text{sech}^2(z)$ models derived from the H -band data at the corresponding radii. Both the scale heights and the relative weights of the two components were taken to be identical to those in the H -band fits at these radii. Only a simple scale factor was applied to the total model profile to match the peak extrapolated brightness of the R -band data. It can be seen that the H -band models provide excellent fits to the R -band data, even at large z values. The small bump near $z = 12''$ in the upper panel is due to an imperfectly subtracted foreground star.

Using two-component $\text{sech}^2(z)$ models, fits were also performed to the R -band brightness cuts at various other galactocentric radii where the H -band profiles had already been fitted. The scale heights of the two components were kept frozen, but the relative weights of the two components was allowed to vary. These models continued to provide excellent fits to the dust-corrected light profiles. As was the case for the H -band data, it was found that it was necessary to increase the light contribution from the larger scale height component as galactocentric radius increased, and that a larger increase was required on the W side of the disk than on the E side.

In spite of the higher signal-to-noise compared with the H -band data at large r , near $|r| \gtrsim 2'.0$ we remain unable to formally distinguish between one-component $\text{sech}(z)$ or $\text{sech}^2(z)$ models and two-component $\text{sech}^2(z)$ model fits, although visually the two-component models appear to retain a slight advantage (Fig. 11). Therefore we cannot rule out that at large galactocentric radii the UGC 7321 is approximately isothermal (but see Section 6.1.1).

5. Caveats, Uncertainties, the Uniqueness of the Fits

Before we discuss the interpretation of the results inferred from fitting the vertical light profiles of UGC 7321, we need to first assess the caveats, uncertainties, and limitations of our fits.

Defining formal errors to the fit parameters we derived for the vertical light structure of UGC 7321 is by no means straightforward (see also Morrison *et al.* 1997; Pohlen *et al.* 2000). In all cases, uncertainties in our fits are expected to arise from systematic effects, including sky subtraction and flatfield errors, Poisson noise, and a host of other factors, such as seeing, finite pixel size, scattered light, and light contamination from background galaxies and field stars. However, it is nearly impossible to formally quantify the magnitude of each of these sources of error, hence we must attempt to make some estimate of their effects indirectly.

In the cases where we have fit our H -band data with a single-component model, we initially fitted both the $+z$ and $-z$ sides of the profiles independently. We found no systematic difference between the scale heights derived for the two halves of the profile. Typically they agreed to within a few per cent, with the maximum difference occurring at $r=0$, where the h_z values derived for both the $+z$ and $-z$ sides of the profile differ by $\sim 10\%$. Although the R -band data at $r = 0$ show a similar result, implying this effect may be real, we conservatively assume the reliability of any individual fit component is $\sim \pm 10\%$. The R -band data have higher signal-to-noise than the H band, but suffer the additional uncertainty from the dust corrections, hence fit errors are expected to be similar in the two bands.

Error assessment is even more complex in cases where we have modelled our light profiles using two-component fits. As discussed by Morrison *et al.* (1997), using one-dimensional fits to galaxy light profiles it is impossible to derive an entirely *unique* decomposition into a multi-component model. Nonetheless, we find it is still possible to derive some simple constraints on the characteristics of the vertical light profile of UGC 7321 using a combination of the present data, $B - R$ color maps (discussed further below), and a few simplifying assumptions.

It would undoubtedly be possible to produce adequate fits the the vertical light profiles of UGC 7321 with more complex models comprised of additional disk components. However, in the present analysis we adopt the simplest models that can fully reproduce our data. Even with a only a two-component model, it is still not possible to determine a completely unique combination of scale heights and relative weightings for the two components to the final fit. However, one can put reasonable limits on both quantities from the present data.

Let us consider the H -band light profiles extracted at $r = \pm 0.5$, and the two-component $\text{sech}^2(z)$ fits derived independently on the $+z$ and $-z$ sides of the profiles, for a total of four independent fits. For each of the four fits, we find empirically that the range of permitted scale heights for the two fit components can be constrained within $\sim \pm 10\%$ by the requirement that the resulting total profile shows both a moderately steep core as well as wings with a statistically significant amplitude at z -heights $|z| \geq 10''$. Likewise, from the fits to the four quadrants, we find

differences of $\lesssim 10\%$ in the mean of the optimum values we derive. Hence in this way, we have estimates of both the intrinsic uncertainties in our fitting approach, as well as uncertainties arising from a range of systematic effects in the data. Thus for the remaining discussion, we assume the uncertainties in the scale heights and relative weightings in our two-component $\text{sech}^2(z)$ model fits to be the sum in quadrature of these two error terms, or $\sim 15\%$.

A final caveat of our present fits is the inability to formally distinguish between models comprised of two $\text{sech}(z)$ rather than two $\text{sech}^2(z)$ components. However, we chose to adopt the $\text{sech}^2(z)$ function (or isothermal disk) due to the fact that it appears to be physically motivated in certain cases (e.g., Dove & Thronson 1993), and has been used to characterize the old disk of the Milky Way (see Freeman 1991), whereas the introduction of the $\text{sech}(z)$ model for galaxy disks was largely based on empirical considerations alone (cf. van der Kruit 1988). Moreover, although the exponential, $\text{sech}(z)$ and $\text{sech}^2(z)$ functions all exhibit very similar behavior at large z , we find that using an exponential for either of our two fit components always produced a model light profile that was too strongly peaked to reproduce our H -band observations at $|r| \leq 0'.25$.

6. Interpretation of the UGC 7321 Fits

6.1. General Considerations

As discussed above, our multi-component fits to the vertical light profiles of UGC 7321 are not necessarily completely unique. What can we therefore say about their physical significance?

Firstly, it is worth noting that the requirement of a minimum of two disk components of differing scale height to reproduce the light profile of UGC 7321 at moderate galactocentric radii establishes that *even a seemingly simple galaxy disk system like UGC 7321 has a complex structure and is not strictly isothermal*. However, greater physical insight can be gleaned by combining the results of our fits with a high-quality $B - R$ color map of UGC 7321. In this way we find that our measurements appear to readily lend themselves to a self-consistent physical interpretation (see Section 6.1.1).

In analyzing the vertical structure of disk galaxies, a number of workers have reported either scale height changes with radius, or else light excesses at large z above those predicted from a single exponential or isothermal disk fit. These have been interpreted as either evidence of a “thick disk” component (e.g., Burstein 1979; van der Kruit & Searle 1981a; Jensen & Thuan 1982; van Dokkum *et al.* 1994; Morrison *et al.* 1997; de Grijs & Peletier 1997), or a possible “halo” component (e.g., Sackett *et al.* 1994; Abe *et al.* 1999). Although these interpretations may well be justified for some galaxies, Dove & Thronson (1993) showed that an alternative in some cases could simply be a disk comprised of a sum of multiple $\text{sech}^2(z)$ components of differing scale heights, where the largest z -height component is the oldest, similar to the early suggestion of Oort (1932), to measurements of the Milky Way (e.g., Freeman 1991 and references therein), and

similar to the models we have proposed for UGC 7321 (see also Kuijken 1991, who proposed an integral representation of components).

To some extent, the differences between the “thick disk” and “multiple component disk” models is one of semantics. However, the distinction is important, since true thick disks analogous to that of the Milky Way (e.g., Gilmore & Reid 1983) are now frequently argued to result from external processes (e.g., Quinn & Goodman 1986; Morrison *et al.* 1998) and thus should not be expected to be present in all disk galaxies. In contrast, a multi-component disk may be a natural consequence of disk heating and other internal evolutionary processes in virtually every galaxy. For a given object, optical color maps can serve as an important aid in distinguishing between these different situations.

6.1.1. Clues from Color Maps

In an analysis of the edge-on galaxy IC 2531, Wainscoat, Freeman, & Hyland (1989) presented a vertical structural study in which color maps were used as an aid to interpreting the light profile fits (see also Jensen & Thuan 1982). In spite of the significant dust lane present in IC 2531, using optical color maps, Wainscoat *et al.* still were able to discern the presence of a very thin, blue, radially extended layer of stars along the galaxy midplane. Based on the existence of this feature, they derived a fit to the disk of IC 2531 using a model comprised of an “old disk” [a large scale-height exponential component ($h_z=533$ pc for $D=22$ Mpc) contributing most of the light], a dust layer, and finally, a “young disk” [a very small scale height exponential component ($h_z=67$ pc) representing the thin layer of blue stars visible in the color maps].

The $B - R$ color map of UGC 7321 is reproduced in Fig. 12, with the location of our vertical light extractions indicated. These data are described in detail in Paper I. Here we review some of the key trends. As discussed in Paper I, a small, red ($B - R \approx 1.5$), nuclear feature is visible at the center of UGC 7321, offset $\sim 5''$ from the isophotal center of the disk. Its nature is enigmatic (Paper I). On either side of this feature, very thin blue bands of stars are visible along the disk midplane, sandwiched in a thicker, much redder region, with $B - R \approx 1.2$. This redder region extends to roughly $\pm 20''$ on either side of the disk center, and then shows a rather abrupt boundary. The intersecting blue layer of stars is seen to change in both color and morphology with radius; in particular, near the edge of the red “sandwich” region, this layer grows rather abruptly and substantially thicker, achieving a roughly constant thickness at radii beyond $\sim \pm 30''$. Beyond that radius, this region grows bluer with radius, reaching $B - R < 0.6$ near the edge of the disk. Finally, out to at least $r \sim \pm 2'.5$, the entire disk of UGC 7321 is surrounded by a thicker but flattened layer of moderately red ($B - R \approx 1.1$) stars.

The complex color structure of the UGC 7321 disk is also evident along the vertical direction. As discussed in Paper I, at $|r| \leq 5''$, vertical color profiles show a reddening of a few tenths of a magnitude in $B - R$ near the galaxy midplane. However, at larger galactocentric radii a

bluing along the galaxy midplane becomes evident. This bluing becomes more pronounced with increasing galactocentric radius, reaching $\Delta(B - R) \sim 0.45$ near $r = 2''.0$. In contrast, at larger z heights ($|z| \gtrsim 7''$), the color stays nearly constant at $B - R \sim 1.1$ over the observed range of galactocentric radii. Here we show that *the features apparent in the $B - R$ color map of UGC 7321 show a number of intriguing correlations with the results of our vertical structure fits.*

6.1.2. Interpretation of the Models at Intermediate Galactic Radii

At galactocentric distances $|r| \geq 0''.5$, we argue that the two $\text{sech}^2(z)$ components required to reproduce the light profile of UGC 7321 represent respectively the blue layer of stars near the midplane and the larger z -height red component visible in our $B - R$ color map. That there is little apparent change in thickness of these two components over the interval $0''.5 \leq |r| \leq 2''.0$ on our color map is consistent with the approximate constancy in scale height of these two components with radius (to within $<10\%$) inferred from our fits. Moreover, the z ranges where each of the respective components is seen to dominate the light distribution in our vertical fits in Fig. 7 & 10 corresponds very closely to the boundaries of these components visible in Fig. 12, or in plots of the vertical color profiles (see Fig. 15 of Paper I). Although we noted in Sections 4.5 & 4.6 that we cannot readily formally distinguish between one- and two-component models at $|r| > 1''.5$, our color map hints that a two-component disk may be present even at these radii.

As mentioned in Sect. 4, our model fits require an increase in the total light contribution of the larger scale-height fit component as a function of radius (see Fig. 7). At first glance this may seem surprising, given that the disk of UGC 7321 gets increasingly *bluer* with radius. One explanation could be that decreasing self-gravity and/or very low surface densities in the outer disk causes a gradual flaring of the star-forming layer, and hence a gradual decrease of the concentration of light in the plane. Indeed, there appears to be evidence of such behavior in *HST* images of UGC 7321 (Gallagher *et al.*, in prep.). However, any subtle change in scale height associated with this would be nearly impossible to infer from our present data, given the decreasing signal-to-noise in the outermost disk regions.

Based on its blue color, it may also seem surprising that the disk component associated with the layer of stars along the disk midplane seems to be prominent even in the H -band data (see Sect. 4.6). Some of this effect likely stems from the fact that the decreased flux of blue stars in the NIR is partially offset by decreased internal absorption at longer wavelengths. Other possibilities are that due to limited dynamical heating in the UGC 7321 disk, this layer contains a mix of stellar populations, including some older, redder stars, or that some NIR flux is emitted by M supergiants (cf. Aoki *et al.* 1991). Indeed, high-resolution imaging data show evidence for populations of young, luminous red supergiants or AGB stars in UGC 7321 (Gallagher *et al.*, in preparation).

As already noted in Paper I, the presence of a redder, unresolved stellar component at larger

z -heights in the UGC 7321 disk seems to give clear evidence that *some dynamical evolution has occurred even in this thin galaxy*. A similar conclusion was reached by Bergvall & Rönback (1995) concerning the superthin galaxy ESO 146-014. Furthermore, our simple double $\text{sech}^2(z)$ model fits are consistent with the suggestion of Dove & Thronson (1993) that the different stellar components of dynamically evolving galaxy disks can indeed be modelled as non-interacting, quasi-independent, isothermal components.

6.1.3. Interpretation of the Models of the Inner Disk Regions

Assuming that the association we infer between our fitted disk components and the vertical color structure of UGC 7321 holds at moderate and large galactic radii, let us now reconsider the disk region near $r=0$. In spite of the deceptively simple, single exponential fit that we derived over the interval $-15'' \leq |r| \lesssim +15''$, closer inspection shows this to be the most structurally complex portion of the UGC 7321 disk.

As seen in Fig. 12, the region of UGC 7321 within $|r| \leq 20''.0$ appears to be comprised of a minimum of three distinct regions: (1) an old disk component like that seen at larger r ; (2) an intermediate thickness redder component, with a rather sharp boundary near $r = \pm 20''$; (3) a very thin blue layer which grows slightly thicker over the interval $0'' < |r| < 20''$, and thereafter appears to flare significantly, blending with the blue disk region described above. Together these components seem to offer a very natural interpretation of the inferred exponential disk structure of UGC 7321 near $r=0$ —i.e., that the disk in this region is comprised of at least three quasi-independent, isothermal or nearly isothermal components: a high z -height component, a moderate z -height component, and a very small scale-height, marginally resolved component along the disk midplane.

Adopting such a model, we can estimate the scale heights of each of these three components in a manner similar to that used at larger galactocentric radii. The determinations were simplified by assuming the highest z height component has a scale height identical to that inferred for the larger z -height component at $r \geq 0'.5$ (~ 423 pc). For the other two components we then estimate $z_0 \approx 2''.4$ (116 pc) and $z_0 \approx 3''.9$ (190 pc). Note that the color map in Fig. 12 shows the thin blue layer to be more strongly defined on the W side of the galaxy than on the E side, which explains why we inferred an exponential disk structure near $r = -15''$, but why the light profile at $r = +15''$ appears to be intermediate between a $\text{sech}(z)$ and an exponential at small z . Note also that this model accounts for the residuals seen in the R -band (and to a lesser degree the H -band) fits at $r = 0$ —i.e., they can be interpreted as a continuation of the larger z -height disk component seen at larger radii.

6.2. Comparison of the Disk Structure of UGC 7321 with the Milky Way and Other Galaxies

6.2.1. The Disk at Moderate Galactocentric Radii

Interpretation of our UGC 7321 data in terms of multiple disk components of differing scale heights (and hence differing characteristic velocity dispersions) is certainly not a new idea. Such components are known to exist in our own Milky Way (see Reid 1993; van der Kruit 1999b for reviews) as well as in other external galaxies (e.g., Jensen & Thuan 1982; Wainscoat *et al.* 1989; van Dokkum *et al.* 1994). Moreover, the existence of disk components with different stellar constituents and characteristic velocity dispersions should be predicted to arise in any galaxy disk via dynamical evolutionary processes (e.g., Fuchs & Wielen 1987; Dove & Thronson 1993; Just *et al.* 1996).

In the galaxy IC 2531, Wainscoat *et al.* (1989) interpreted the small scale-height, blue layer of stars seen along the disk midplane as a disk component analogous to the Milky Way’s “young disk”. This layer is thus presumably comprised primarily of OB stars, gas, and dust. Wainscoat *et al.* (1989) interpreted the underlying larger z -height disk component as analogous to the Milky Way’s “old disk”. It is presumed to be comprised of older, redder, lower mass stars (see also Jensen & Thuan 1982; van Dokkum *et al.* 1994). Indeed, based on their respective scale heights and colors, a similar interpretation seems natural for the disk components we infer at intermediate radii in UGC 7321. Thus at intermediate galactocentric radii, UGC 7321 can be said to have an “old disk” with scale height $z_{0,O} \approx 423$ pc, and a “young disk” with scale height $z_{0,Y} \approx 185$ pc.

In their analysis of IC 2531, Wainscoat *et al.* used exponential rather than $\text{sech}^2(z)$ fits⁶; thus recalling the relation $z_0 = 2h_z$, we see that to within distance uncertainties, the scale height we measure for the young disk of UGC 7321 is comparable to that of IC 2531 ($h_z \sim 67$ pc) and of the Milky Way ($h_z \sim 100$ pc; Reid 1993; van der Kruit 1999b). However, the “old disk” of UGC 7321 is considerably thinner compared with $h_z \approx 533$ pc measured for the old disk of IC 2531 (Wainscoat *et al.* 1989), $z_0 \approx 1.1$ kpc for NGC 6504 (van Dokkum *et al.* 1994; see also de Grijs 1997 and references therein), and $h_z \sim 325$ pc for the Milky Way (Reid 1993). Existing measurements thus seem consistent with the actively star-forming disks of most disk galaxies having roughly similar scale heights, while the differences in their global scale heights mainly stem from differences in the thicknesses of their older stellar components.

The old disks of galaxies are expected to be formed from stars that have been scattered to higher z -heights via interactions with giant molecular clouds or scattering from spiral arms (see Freeman 1991). Mild interactions should also act to heat disks, at least temporarily (e.g.,

⁶Note there is no inconsistency here with our double $\text{sech}^2(z)$ models of UGC 7321, since observations of K giants in the Milky Way have shown that its old disk is indeed isothermal to at least 450 pc above the plane, while the apparent overall exponential nature of the disk results from the presence of additional dynamically colder stellar populations (Freeman 1993).

Reshetnikov & Combes 1997). Hence it is not surprising that compared to normal spirals, the old disk should be significantly thinner in an isolated “superthin” galaxy like UGC 7321. One obvious conclusion is then that UGC 7321 has undergone less dynamical heating and evolution than spirals like the Milky Way or IC 2531.

Some galaxy formation models predict that galaxies that are built very slowly over time are expected to have very thin disks (e.g., Dove & Thronson 1993; Noguchi 1998). While a long formation timescale may be a required condition for the formation of a superthin galaxy, our present results seem to indicate that the superthin appearance of UGC 7321 is not solely a result of the conditions of formation, but also a consequence of having avoided significant subsequent dynamical heating. This lack of heating could be due to the low density of its disk, the lack of large molecular complexes or spiral arms to scatter stars, the presence of an unusually massive dark matter halo, and/or the consequence of having remained isolated during most of its lifetime.

One last point worth noting is that the relative light contribution of the young disk compared to the old disk that we infer for UGC 7321 is considerably higher than that derived for galaxies such as IC 2531 or the Milky Way. However, such a trend seems as expected for a blue, gas-rich, low surface brightness galaxy like UGC 7321, where past star formation has likely been low, heating of older populations has presumably been mild, and where the global disk colors are dominated by fairly young stars.

6.2.2. The Inner Disk Regions

As discussed in Sect. 6.1.3, at least two additional disk components appear to be present in UGC 7321 at small galactocentric radii ($|r| \leq 20''$) in addition to the old stellar disk: an intermediate scale-height component with $z_0 \sim 190$ pc and a very thin component with $z_0 \sim 116$ pc.

The bulk of the very small scale height component in the inner regions of UGC 7321 ($|r| \lesssim 15''$) has a blue color and gives rise to the observed globally exponential nature of the vertical light profile near the galaxy center. This may be a distinct disk region of UGC 7321, or it could be simply an extension of UGC 7321’s star-forming disk from larger radii, but where the scale height has become dramatically smaller due to the larger self-gravity near the disk center. As noted above, near the center of this region, a rather compact red feature ($\sim 5''$ across) is seen in our color maps. This too may be a distinct disk subcomponent, although it does not add any distinguishable feature to the vertical light profiles. The extent of this feature (~ 200 pc) is similar to that of the CO-rich “nuclear disk” regions of the Milky Way or NGC 891, where $R \sim 225$ pc (Scoville *et al.* 1993). In the Milky Way, the nuclear disk has a FWHM thickness of ~ 65 pc (Scoville *et al.* 1993)—similar to the apparent extent of the feature in UGC 7321. Although CO has recently been detected from the central regions of UGC 7321 (Matthews & Gao, in preparation), the resolution is insufficient to map its spatial distribution. We therefore collectively refer to this small scale-height red feature and the surrounding small scale-height blue disk seen at $|r| \lesssim 15''$ as

the “young nuclear disk” of UGC 7321.

Lastly, we comment on the red disk region seen in UGC 7321 at $|r| \lesssim 20''$ (1 kpc). It was shown in Paper I that this region corresponds very closely in radial extent to a light excess over a radial purely exponential brightness profile (see also Fig. 2). In a less inclined spiral, such a light excess would normally be interpreted as evidence for a bulge. However, such an interpretation seems highly questionable for the case of UGC 7321, which shows little central concentration of light in broad-band images, and whose disk does not appear to “bulge” at all (e.g., Fig. 1). However, since it is now believed that the bulges of late-type disk galaxies form from inner disk instabilities (e.g., Combes *et al.* 1990; Norman, Hasan, & Sellwood 1996; Carollo 1999), one possible explanation for this region is that it corresponds to some type of “proto-bulge”. Although this is only one possible interpretation (see Paper I), we shall henceforth use this term to refer to this disk component of UGC 7321.

6.2.3. Summary of Disk Components in UGC 7321

To summarize, in spite of its “underevolved” appearance, UGC 7321 has a complex disk structure, with as many as 4 distinct components of differing scale height (and hence of differing characteristic velocity dispersions) and differing stellar make-up (as evidenced by their different $B - R$ colors and differing radial extents). We term these: (1) the *old disk* with $z_{0,O} \approx 423$ pc; (2) the *young disk* with $z_{0,Y} \approx 185$ pc; (3) the *young nuclear disk* with $z_{0,N} \approx 116$ pc; (4) the *proto-bulge* with $z_{0,P} \approx 190$ pc. The observed superposition of all the disk components near $r = 0$ yields an approximately exponential light distribution with a *global* exponential scale height of $h_{z,g} \approx 140$ pc. These results are consistent with a scenario where the exponential nature of the vertical light profile of galaxy disks is a result of dynamical evolution rather than purely the conditions of its formation.

7. Estimating the Vertical Velocity Dispersion in UGC 7321

Measures of vertical velocity dispersions (σ_z) are of enormous interest in studies of disk galaxies, since they can be used to gauge the vertical stability of disks (e.g., Fridman & Polyachenko 1984) and permit determinations of the stellar mass-to-light ratio Υ_* , which in turn allows a determination of the total mass contribution of the stellar disk. This is critical for interpreting galaxy rotation curves in terms of mass models such that the quantity and distribution of dark matter can be inferred.

Unfortunately, stellar velocity dispersion measurements are quite challenging observationally, hence they have been obtained only for a handful of nearby disk galaxies (e.g., Bottema 1993 and references therein). For this reason, it is of interest to attempt to estimate σ_z indirectly, using measures of the disk scale height, luminosity, and rotational velocity (e.g., Bottema 1993, 1997; van

der Kruit 1999a). We now have the data to attempt this exercise for UGC 7321. For simplicity, we limit ourselves to computing mean velocity dispersions using the global disk scale heights from the single-component fits in Section 4.4.

For a disk with an exponential brightness profile, the vertical velocity dispersion can be expressed as

$$\sigma_z(r) = \left[4\pi G h_z \Sigma(r) \left(1 - \frac{1}{2} e^{-|z|/h_z} \right) \right]^{1/2} \quad (7)$$

where $\Sigma(r)$ is the mass surface density at a given radius and G is the gravitational constant (Wainscoat, Freeman, & Hyland 1989). For a $\text{sech}(z)$ vertical brightness distribution, one has instead

$$\sigma_z(r) = [1.7051\pi G \Sigma(r) h_z]^{1/2}. \quad (8)$$

(e.g., van der Kruit 1999a).

One approach to estimating σ_z involves assuming a reasonable value for Υ_* and converting the measured stellar surface density to a mass density. However, this is particularly uncertain for an LSB galaxy like UGC 7321, which has strong radial and vertical color gradients and an uncertain metallicity. Instead we therefore adopt the approach of van der Kruit (1999a), whereby the disk is assumed to be globally stabilized by a dark halo. In that case, the semi-empirical criterion for global stability of Efstathiou *et al.* (1982):

$$V_{rot} \left(\frac{h_r}{GM_{disk}} \right)^{1/2} \lesssim 1.1. \quad (9)$$

may be applied to estimate a total disk mass M_{disk} .

For UGC 7321, we have $V_{rot} \approx \frac{1}{2}(W_{20} - 20) = 106 \text{ km s}^{-1}$ (where we have corrected the measured global HI linewidth from Table 1 for turbulence; see Matthews, van Driel, & Gallagher 1998). Using the above relation, we derive $M_{disk} \approx 4.5 \times 10^9 \mathcal{M}_\odot$. With the additional approximation that the HI follows the same distribution as the stars, we can subtract the mass contribution for the HI, corrected for He, and arrive at $\Sigma(0) \approx 110 \mathcal{M}_\odot \text{ pc}^{-2}$. At $r = 0$, taking $h_z = 140 \text{ pc}$ and using Equation 7 yields $\sigma_z(0) \sim 20.4 \text{ km s}^{-1}$. At $r = 0.5$, using a mean $h_z = 145 \text{ pc}$ and assuming $\Sigma(R) = \Sigma(0)e^{-r/h_r}$, from Equation 8 we get $\sigma_z(0.5) \sim 13.7 \text{ km s}^{-1}$, and at $r = 1h_r$, $\sigma_z(1h_r) \sim 12.3 \text{ km s}^{-1}$. These values imply that UGC 7321 is a very dynamically cold galaxy (cf. Bottema 1993). In spite of the approximations we have used, our σ_z estimates show good agreement with the *measured* values from Swaters (1999) for the moderately LSB dwarf spiral galaxy UGC 4325. He finds $\sigma_z(0) \sim 19 \text{ km s}^{-1}$ and $\sigma_z(1h_r) \sim 13 \text{ km s}^{-1}$ (although note the measured σ_z values are due to all mass components of the galaxy, not just the stars). With $M_B = -17.5$ and $h_r = 1.6 \text{ kpc}$, UGC 4325 has a size and luminosity similar to UGC 7321, hence it is indeed expected that these two systems should have similar stellar velocity dispersions (e.g., Bottema 1993).

8. Summary

We have presented measurements of the vertical structure of the low-luminosity “superthin” spiral galaxy UGC 7321. Using a combination of H - and R -band data and $B - R$ color maps, we find that like more luminous disk galaxies, UGC 7321 has a complex, multi-component disk structure, indicating that some dynamical heating has occurred even in this thin galaxy. Our analysis has demonstrated the power of high-resolution color maps as an aid in interpreting disk structural measures (see also Jensen & Thuan 1982; Wainscoat *et al.* 1989). Our findings for UGC 7321 also underscore the importance of utilizing high resolution, multiwavelength data and sampling the full range of z -heights of a galaxy disk when assessing its vertical structure (see also Dove & Thronson 1993).

Near the disk center, the global H - and R -band vertical light profiles of UGC 7321 can be reasonably characterized by a single exponential function. We derive a global scale height at the disk center ($r = 0$) of $h_{z,g,H} \approx 140 \pm 15$ pc in H -band and $h_{z,g,R} \approx 152 \pm 15$ pc in R -band. These are among the smallest global vertical scale heights ever reported for any galaxy disk, implying that UGC 7321 has not only a large disk axial ratio, but also an intrinsically thin disk. Its distance-independent ratio $h_r/h_z \sim 14$ (at $r = 0$) is also among the largest reported for a galaxy disk. The overall exponential appearance of the UGC 7321 disk at small galactocentric radii appears to result from the superposition of at least three quasi-independent isothermal or nearly isothermal disk components of differing scale heights: (1) an “old disk” with $z_{0,O} \approx 423$ pc; (2) a “young nuclear disk” with $z_{0,N} \approx 116$ pc; (3) a “proto-bulge” with $z_{0,P} \approx 190$ pc. Near the disk center, we estimate a mean stellar velocity dispersion of $\sigma_z(0) \sim 20$ km s⁻¹.

At roughly $20''$ (1 kpc) from the galaxy center, the vertical light profile of UGC 7321 becomes less peaked than an exponential near the midplane. At $|r| \geq 20''$, although a $\text{sech}(z)$ function can provide a rough global characterization of the data, we find the best fits to the observed H - and R -band light profiles are produced by a linear combination of two isothermal components, one representing a continuation of the “old disk” with $z_{0,O} \approx 423$ pc, and the other a “young disk” component with $z_{0,Y} \approx 185$ pc. Both seem to contribute roughly equal fractions to the total light in both the H and R bands, although the contribution of the old disk component increases slightly as a function of galactocentric radius. Using this model we find no evidence for a significant change in disk scale height as a function of radius over the interval $15'' \leq |r| \leq 2'0$, although we cannot rule out changes of $<10\%$. From our present data it is unclear whether the “young nuclear disk” is a distinct entity, or whether it may be an extension of the young disk to small galactocentric radii, where higher self-gravity results in a dramatically smaller scale height. At $|r| \geq 2'0$ our $B - R$ color map suggests a continuation of a multi-component disk structure, although formal fits cannot rule out one-component models, suggesting the possibility that the disk may become nearly isothermal or $\text{sech}(z)$ -like at large galactocentric radii. If we use a single-component model to characterize the disk at these radii, we find that near $|r|=2'0$ the ratio of disk scale height to scale length becomes $h_r/h_z \sim 10$, or roughly one-third smaller than at $r=0$.

The mean scale height of the young disk of UGC 7321 is comparable to that of the Milky Way and other external galaxies, suggesting that the thickness of the star-forming layer in most spirals may be roughly similar. The colors and z distribution of the old disk component of UGC 7321 are consistent with it being comprised of an older population of stars that have acquired higher velocity dispersions over time. However, the inferred scale height of UGC 7321’s old disk is significantly lower than that of most spiral galaxies measured to date. Thus while some dynamical heating has occurred in UGC 7321, it appears to have been extremely limited compared with typical giant spirals. Results presented here and in Paper I seem to suggest that isolation, a low disk surface density, and a massive dark matter halo are key requirements for UGC 7321 to maintain its svelte appearance. Important additional tests of these hypotheses will require stellar velocity dispersion measurements and detailed mass modelling of galaxies like UGC 7321.

I am grateful for the financial support provided by a Jansky Postdoctoral Fellowship from the National Radio Astronomy Observatory. I acknowledge useful discussions with J. S. Gallagher, L. S. Sparke, and B. Fuchs on various portions of this work, and I thank an anonymous referee for valuable comments. This publication made use of data products from the Two Micron All Sky Survey, which is a joint project of the University of Massachusetts and the Infrared Processing and Analysis Center/California Institute of Technology, funded by the National Aeronautics and Space Administration and the National Science Foundation.

REFERENCES

- Abe, F. *et al.* 1999, *AJ*, 118, 261
- Abramowitz, M. & Stegun, I. A. 1965, *Handbook of Mathematical Functions*, (New York: Dover)
- Aoki, T. E., Hiromoto, N., Takami, H., & Okamura, S. 1991, *PASJ*, 43, 755
- Barnaby, D. & Thronson, H. A. Jr. 1992, *AJ*, 103, 41
- Barteldrees, A. & Dettmar, R.-J. 1994, *A&AS*, 103, 475
- Bergvall, N. & Rönnback, J. 1995, *MNRAS*, 273, 603
- Bevington, P. R. 1969, *Data Reduction and Error Analysis for the Physical Sciences*, (New York: McGraw-Hill)
- Bothun, G., Impey, C., & McGaugh, S. 1997, *PASP*, 109, 745
- Bottema, R. 1993, *A&A*, 275, 16
- Bottema, R. 1997, *A&A*, 328, 517
- Burkert, A. & Yoshii, Y. 1996, *MNRAS*, 282, 1349
- Burstein, D. 1979, *ApJ*, 234, 829
- Capaccioli, M., Vietri, M., & Held, E. V. 1988, *MNRAS*, 234, 335
- Carollo, C. M. 1999, *ApJ*, 523, 566
- Chatterjee, S. & Price, B. 1977, *Regression Analysis by Example*, (New York: John Wiley & Sons)
- Combes, F., Debbasch, F., Friedl, D., & Pfenniger, D. 1990, *A&A*, 233, 82
- de Grijs, R. 1997, Ph.D. thesis, University of Groningen
- de Grijs, R. 1998, *MNRAS*, 299, 595
- de Grijs, R. & Peletier, R. F. 1997, *A&A*, 320, 21
- de Grijs, R., Peletier, R. F., & van der Kruit, P. C. 1997, *A&A*, 327, 966
- Dove, J. B. & Thronson, H. A. 1993, *ApJ*, 411, 632
- Efstathiou, G., Lake, G., & Negroponte, J. 1982, *MNRAS*, 199, 1069
- Freeman, K. C. 1991, in *Dynamics of Disc Galaxies*, edited by B. Sundelius, (Göteborg: Göteborgs University and Chalmers University of Technology), 15
- Freeman, K. C. 1993, in *Galaxy Evolution: The Milky Way Perspective*, ASP Conference Series, Vol. 49, edited by S. R. Majewski, (San Francisco: ASP), 125
- Fridman, A. M. & Polyachenko, V. L. 1984, *Physics of Gravitating Systems*, (New York: Springer-Verlag)
- Fry, A. M., Morrison, H. L., Harding, P., & Boroson, T. A. 1999, *AJ*, 118, 1209
- Fuchs, B. & Wielen, R. 1987, in *The Galaxy*, Proceedings of the NATO Advanced Study Institute, Cambridge, England, edited by G. Gilmore, and R. Carswell, (Dordrecht: Reidel), 375

- Gilmore, G. & Reid, N. 1983, MNRAS, 202, 1025
- Howk, J. C. & Savage, B. D. 1999, AJ, 117, 2077
- Jensen, E. B. & Thuan, T. X. 1982, ApJS, 50, 421
- Just, A., Fuchs, B., & Wielen, R. 1996, A&A, 309, 715
- Knapen, J. H. & van der Kruit, P. C. 1991, A&A, 248, 57
- Kodaira, K. & Yamashita, T. 1996, PASJ, 48, 581
- Kuijken, K. 1991, ApJ, 372, 125
- Matthews, L. D. 1998, Ph.D. Thesis, State University of New York at Stony Brook
- Matthews, L. D. & Gallagher, J. S. 1997, AJ, 114, 1899
- Matthews, L. D., Gallagher, J. S., & van Driel, W. 1999, AJ, 118, 2751 (Paper I)
- Matthews, L. D., van Driel, W., & Gallagher, J. S. 1998, AJ, 116, 2196
- Moffat, A. F. J. 1969, A&A, 324, 80
- Morrison, H. L., Fry, A. M., Harding, P., Boroson, T., Stinebring, D., & Miller, E. 1998, AAS, 193.817
- Morrison, H. L., Miller, E. D., Harding, P., Stinebring, D. R., & Boroson, T. A. 1997, AJ, 113, 2061
- Noguchi, M. 1998, Nature, 392, 253
- Norman, C. A., Sellwood, J. A., & Hasan, H. 1996, ApJ, 462, 114
- Oort, J. H. 1932, Bull. Astron. Inst. Netherlands, 6, 249
- Pohlen, M., Dettmar, R.-J., Lütticke, R., & Schwarzkopf, U. 1999, preprint
- Pritchett, C. 1983, AJ, 88, 1476
- Quinn, P. J. & Goodman, J. 1986, ApJ, 309, 472
- Reid, N. 1993, in *Galaxy Evolution: The Milky Way Perspective*, edited by S. R. Majewski, ASP Conference Series, Vol. 49, (San Francisco: ASP), 37
- Reshetnikov, V. & Combes, F. 1997, A&A, 324, 80
- Rice, W., Merrill, K. M., Gatley, I., & Gillett, F. C. 1996, AJ, 112, 114
- Sackett, P. D., Morrison, H. L., Harding, P., & Boroson, T. A. 1994, Nature, 370, 441
- Saglia, R. P., Bertschinger, E., Bagley, G., Burstein, D., Colless, M., Davies, R. L., McMahan, R. K. Jr., & Wegner, G. 1993, MNRAS, 264, 961
- Scoville, N. Z., Thakkar, D., Carlstrom, J. E., & Sargent, A. I. 1993, ApJ, 404, L59
- Spitzer, L. 1942, ApJ, 95, 329
- Swaters, R. A. 1999, Ph.D. Thesis, University of Groningen

- Tully, R. B., Shaya, E. J., & Pierce, M. J. 1992, *ApJS*, 80, 479
- van der Kruit, P. C. 1988, *A&A*, 192, 117
- van der Kruit, P. C. 1999a, in *Toward a New Millenium in Galaxy Morphology*, edited by D. L. Block, in press
- van der Kruit, P. C. 1999b, in *the Legacy of J. C. Kapteyn: Studies on Kapteyn and the Development of Modern Astronomy*, edited by P.C. van der Kruit & K. van Berkel, 299, in press
- van der Kruit, P. C. & Searle, L. 1981a, *A&A*, 95, 105
- van der Kruit, P. C. & Searle, L. 1981b, *A&A*, 95, 116
- van der Kruit, P. C. & Searle, L. 1982a, *A&A*, 110, 61
- van der Kruit, P. C. & Searle, L. 1982b, *A&A*, 110, 79
- van Dokkum, P. G., Peletier, R. F., de Grijs, R., & Balcells, M. 1994, *A&A*, 286, 415
- Wainscoat, R. J., Freeman, K. C., & Hyland, A. R. 1989, *ApJ*, 337, 163
- Zasov, A. V., Makarov, D. I., & Mikhailova, E. A. 1991, *Sov. Astron. Lett.*, 12, 374

Fig. 1.— *R*-band image of UGC 7321 obtained with the WIYN telescope (see Paper I for details). The image is $\sim 6' \times 1'$. North is on top, west on the left. Overplotted are pluses indicating the location of the extracted vertical light profiles analyzed in this paper. The larger symbol denotes the galaxy center ($r=0$).

Fig. 2.— Radial surface brightness profiles in mag arcsec^{-2} along the major axis of UGC 7321: *H*-band (top); *R*-band (center); *B*-band (bottom). The data were extracted along the disk major axis and folded about $r=0$, as described in Section 3. Exponential fits to each of the profiles are overplotted as dashed lines. The *H*-band data shown are not photometrically calibrated, hence the absolute surface brightness scale for these data was estimated using the *H*-band data from the Two Micron All Sky Survey (see Text), and was then offset by $+1 \text{ mag arcsec}^{-2}$ for display purposes.

Fig. 3.— *H*-band minor axis light profile of UGC 7321. The absolute photometric calibration was estimated using *H*-band data from the Two Micron All Sky Survey (see Text). Data points are shown as plus signs. The best-fitting exponential model fits are overplotted as dashed lines. Error bars were estimated as a sum in quadrature of Poisson, flatfield, and sky subtraction errors.

Fig. 4.— As in Fig. 3, but at $r = -15''$ (top) and $r = +15''$ (bottom). In the lower panel a $\text{sech}(z)$ fit has also been plotted as a solid line. Note in the lower panel that the exponential fits are too peaked to reproduce the data at small z , while the $\text{sech}(z)$ fit is somewhat too rounded at small z and underestimates the profile wings at large z .

Fig. 5.— As in Fig. 3, but at $r = -0.5$ (top) and $r = +0.5$ (bottom). Here the best-fitting exponential fits are shown as short dashed lines, the best-fitting $\text{sech}(z)$ functions as solid lines, and the best $\text{sech}^2(z)$ models as long dashed lines.

Fig. 6.— *H*-band light profiles extracted parallel to the minor axis of UGC 7321 at various galactocentric radii. The best-fitting $\text{sech}(z)$ fits are overplotted. The panels depict light profiles extracted at the following locations: (a): $r = -0.5$ (top); $r = +0.5$ (bottom); (b): $r = -1.0$ (top); $r = +1.0$ (bottom); (c): $r = -1.5$ (top); $r = +1.5$ (bottom); (d): $r = +2.0$. Error bars were estimated as in Fig. 3.

Fig. 7.— As in Fig. 5, but with model fits comprised of two $\text{sech}^2(z)$ functions of scale heights $z_0 = 3''.8$ and $z_0 = 8''.7$ respectively overplotted as long dashed lines. The contribution of each of the two components to the total light is indicated by short dashed lines.

Fig. 8.— *R*-band minor axis profile of UGC 7321. The data are shown as plus signs. The dotted line shows the data after correction for dust absorption (see Text). The dashed lines show the best-fitting exponential functions. Error were estimated using a quadratic sum of Poisson, flatfield, and sky subtraction errors and do not account for uncertainties in the correction for dust absorption. Error bars are plotted only for every tenth data point.

Fig. 9.— *R*-band vertical light profiles extracted at $r = -0.5$ (top) and $r = +0.5$ (bottom). The

dotted lines show estimates of dust-corrected profiles. The solid lines are the $\text{sech}(z)$ fits derived from the H -band data at these respective radii. Error bars are plotted only for every tenth data point.

Fig. 10.— As in Fig. 9, but with model fits comprised of two $\text{sech}^2(z)$ functions of scale heights $z_0 = 3''.8$ and $z_0 = 8''.7$, respectively, overplotted as long dashed lines. The contribution of each of the two components to the total light is indicated by a short dashed line. The bump near $z = 12''$ in panel (a) is due to an imperfectly-subtracted foreground star.

Fig. 11.— R -band vertical light profiles at $r = -2'.0$ (top) and $r = +2'.0$ (bottom). The solid lines show the best $\text{sech}(z)$ fits. The long dashed line shows the best single-component $\text{sech}^2(z)$ fit. The thick, medium dashed line shows a two-component $\text{sech}^2(z)$ model with $z_{0,1} = 3''.8$ and $z_{0,2} = 8''.7$; the contributions of the two components are overplotted as short dashed lines.

Fig. 12.— Pseudocolor $B - R$ color map obtained from the WIYN imaging data of Paper I. Seeing was $\sim 0''.6$. Locations where the vertical light profiles were extracted and analyzed in the present paper are marked by pluses. In this color scheme, the intrinsically reddest regions of the disk ($B - R > 1.5$) are seen as yellow. Other colors translate as follows: reddish-orange ($B - R \sim 1.2$); greenish black ($B - R \sim 1.1$); purple ($B - R \sim 1.0$); blue ($B - R \sim 0.8$); black ($B - R < 0.7$). The field of view shows roughly the inner $3'.8$ of the disk. $r = 0$ is at the image center and is indicated by the symbol just to the left of the small yellow feature.